Optical and Quantum Electronics (2023) 55:123
https://doi.org/10.1007/s11082-022-04325-z

Room temperature ferromagnetism in metal oxides for spintronics: a comprehensive review

Sundar Singh[1] · Veerendra Kumar[1] · Sanjeev Tyagi[2] · Nupur Saxena[3] · Zishan H. Khan[4] · Pragati Kumar[5]

Received: 4 August 2022 / Accepted: 22 October 2022
© The Author(s), under exclusive licence to Springer Science+Business Media, LLC, part of Springer Nature 2022

Abstract
This review presents a comprehensive account of the research scenario in the ferromagnetic (FM) behavior displayed at room temperatures (RT) in the metal oxides (MOx) for spintronics applications. Spintronic devices need simultaneous manipulation of charge and spin of the electron and the material needed for the fabrication of such devices must show the existence of FM behavior at or above RT. This article discusses the induction of room temperature FM (RTFM) behavior in MOx via doping and co-doping of magnetic and non-magnetic ions. The semiconductor doped with magnetic ions (usually up to maximum 10%) are well known as dilute magnetic semiconductors (DMSs) whereas they are known as d^0 FM materials with doping of non-magnetic ions. This review mainly focuses on the MOx based DMSs. The various mechanisms and models for the induction of RTFM in such systems are discussed followed by their advantages and drawbacks along with their technological applications. However, a short discussion on RTFM behaviors of d^0 materials is also presented. Further, the influence of various morphologies on RTFM behavior of MOx followed by the RTFM in *2D*-MOx is also discussed.

Keywords Dilute magnetic semiconductors · Transition metals · d^0 materials · 2D-MOx · RTFM · Spintronics

✉ Sundar Singh
ssg01bcb@gmail.com

✉ Pragati Kumar
pkumar.phy@gmail.com

[1] Department of Physics, Bareilly College, Bareilly 243005, India

[2] Department of Electronics and Instrumentation Engineering, MJP Rohilkhand University, Bareilly 243006, India

[3] Organisation for Science Innovations and Research, Bah 283104, India

[4] Department of Applied Sciences and Humanities, Jamia Millia Islamia (Central University), New Delhi 110025, India

[5] Nano-Materials and Device Lab, Department of Nanosciences and Materials, Central University of Jammu, Rahya Suchani, Samba, Jammu 181143, India

Published online: 17 December 2022

1 Introduction

Requirements of ever increasing storage density, fast processing speed and lesser power consumption by the electronic devices have created the need to replace the currently used charge-based electronics with the spin-based electronics or spintronics. The search for the synthesis and identification of new magnetic materials has been intensified to invent the novel spintronic devices, which utilize spin degrees of freedom along with the charge of electrons. Due to the peculiar feature of effective manipulation of the charge and spin in the magnetic semiconductors, these materials are seen to be highly suitable for the development of the devices combining logic functionalities and the information storage capabilities (Liu et al. 2016). So far, the best known materials suitable for the development of spintronic devices are the ferromagnetic semiconductors, better known as the dilute magnetic semiconductors (DMSs), which are the semiconducting materials (III-V, II-VI, or IV-IV) with the doping of magnetic or non-magnetic transition metal ions (TM ions such as Cr, Fe, Co, Ni, Mn, V, and Cu etc.) typically up to maximum 10% (Boscherini 2008). In DMSs, also called semi-magnetic semiconductors, the dopant atoms (ions) replace some of the atoms (ions) from the host lattice and acquire high magnetic moments (MMs). Due to the presence of both semiconductor as well as magnetic impurity atoms, DMSs exhibit properties, which are characteristic of both the semiconductors as well as magnetic materials. Notable among these are the properties of magnetoelectricity and ferromagnetism (FM); more importantly FM at/or above room temperature (RT). The physical properties such as energy band gap or MMs of these magnetic semiconductors are not only the function of particle size but also depend upon the doping level of magnetic atoms/ions. The distinctive material characteristics such as the spin-dependent coupling between semiconductor bands and the localized states of the magnetic ions promises the magnetoelectric effect i.e. the variation of magnetic properties by an applied electric field or induction of magnetization due to the application of electric field in non-magnetic materials (Wang et al. 2011).

For the information storage and other device applications, the FM shown by the material must exist at RT. Although successful doping of TM in III-V (particularly, Mn in GaAs) semiconductors could be achieved, but the FM shown by these systems was at temperatures much below RT, thus couldn't make these materials suitable for spintronics applications. The first theoretical prediction of RTFM in DMSs provided impetus to the scientific world for the greater exploration of these materials experimentally (Dietl et al. 2000). Afterwards, a great deal of interest in DMSs materials arose in the scientific community because of the prediction of FM above RT in highly (p-type) Mn-doped wurtzite structured ZnO and GaN (Bhandarkar Lata 2014; Bououdina et al. 2014; Ahmed 2017; Han and Park 2005; Li et al. 2009). In DMSs, spin and charge degrees of freedom of charge carriers can be independently tuned for realizing multifunctional devices. DMSs have gained significant attention among researchers in view of their potential applications in spintronic, optoelectronic, photocatalytic, photovoltaic and magnetoelectronic devices (Kim and Park 2002; Du et al. 2008; Zhang et al. 2017; Sheng et al. 2016). Besides, DMSs also find applications in spin polarized light emitting devices (spin-LEDs), spin field effect transistors (spin-FETs), as an anode material in lithium-ion batteries, non-volatile memory storage (MRAM), logic devices, ultrafast optical switches, dye-sensitized solar cells (DSSCs), quantum computers etc. (Sharma et al. 2003; Mahmoud 2010; Mahmoud et al. 2012). Potential spintronic and magneto-optic applications of DMSs have been targeted by the investigation of RTFM due to the addition of TM atoms in the semiconductors. The RTFM has been observed in the

broad range of materials including metal oxides (MOx), metal chalcogenides (MChs), carbon nanostructures (NSs), 2D materials, Maxene, and perovskites etc. (Xing et al. 2009a; Ghosh et al. 2013; Wu et al. 2021; Morozov et al. 2021; Tsai et al. 2021; Wang et al. 2009; Tan et al. 2021; Zhou et al. 2021; Alam and Mandal 2020; Iqbal et al. 2020). However, MOx like TiO_2, ZnO, SnO_2, CuO and In_2O_3 etc. have been widely and persistently explored for their potential spintronic applications. MOx possess wide-ranging optical, electronic, and chemical properties along with the ease of fabrication as compared to the conventional non-oxide counterparts therefore earning them the status of potential materials for a variety of practical device applications (Nagal et al. 2020; Khan et al. 2010). Besides, the environmental friendly nature with high chemical stability and low processing cost of MOx make them superior to other materials (Salah et al. 2011). Though, RTFM has been observed in sole MOx NSs but the induced/developed MMs are small and insufficient for practical applications (Kumar et al. 2022). The RTFM behavior is broadly manipulated via doping and co-doping of magnetic and non-magnetic (particularly TM) elements. TM doping in MOx is found to increase the number of crystal defects and thereby improves their optical as well as magnetic properties (Azam et al. 2013). Because of the above mentioned advantages of MOx, the researchers are exploring them to achieve new dimensions in the field of DMSs and the frequency of publications on MOx based RTFM is still more than 30% of total publication (Fig. 1). The Fig. 1 clearly illustrates that to date only ZnO contributes around 10% of publication on DMS. This article presents a brief discussion on the suitability, adaptability, and compatibility of extensively used MOx towards achieving RTFM for spintronic applications.

2 Different oxides based DMSs systems

TM doped TiO_2, ZnO, SnO_2, CuO and In_2O_3 are the prominent oxide-based DMSs materials which have been extensively investigated for the occurrence of RTFM keeping in view their prospective applications in the field of spintronics.

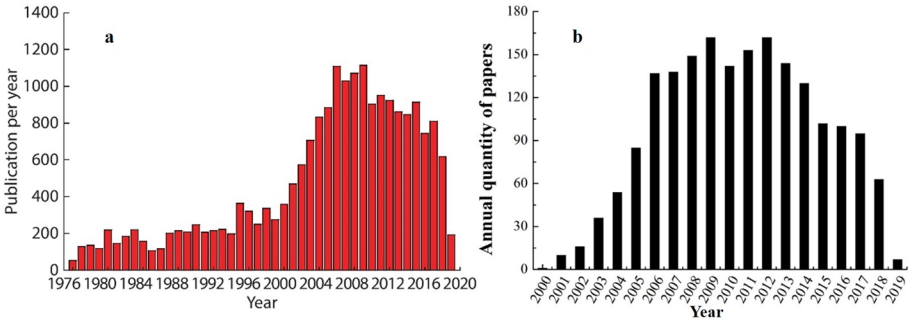

Fig. 1 Year wise frequency of research publications on diluted magnetic semiconductors based on **a** various materials (Cao and Yan 2019) and **b** ZnO (Li et al. 2019)

2.1 Single ion doped DMS systems

2.1.1 RTFM in TiO_2-based DMSs

The research into the field of oxide-based DMSs was initiated by the observance of ferromagnetic behavior above RT in the Co-doped TiO_2 (Matsumoto et al. 2001). TiO_2, a wide band gap ($\approx 3.2eV$) n-type semiconductor can be used as a DMSs due to the manifestation of distinctive ferromagnetic behaviour. For TiO_2 nanocrystals several synthesis techniques are possible. These include sol–gel technique, hydrothermal method, chemical vapour deposition (CVD), electrochemical coating etc.

The potential use of TiO_2 as DMSs is inspired by its good optical transmission at UV-visible and near infrared wavelengths. TiO_2 nanocrystals have been extensively researched due to their non-toxic nature, facile low-cost synthesis, great stability values, and exotic electronic, optical and magnetic properties. Further, the improvement in saturation magnetization and the possibility of tailoring the band gap provides interesting features required for the magneto-optoelectronic applications. The range of magnetic properties shown by TiO_2 DMS is dependent on the type of dopant TM ions. Magnetic characteristics of DMS materials include paramagnetism (PM), diamagnetism (DM), FM as well as superparamagnetism (SPM). However, for the purpose of spintronic applications, FM behavior at RT is the essential trait in the material. The presence of defects in TiO_2-based DMS is shown to be responsible for the magnetic behavior shown by these materials (Santara et al. 2014). TM-doped TiO_2 showcases RTFM not only in the thin films but also in the form of nanoparticles (NPs) and other NSs (Mudarra Navarro et al. 2014).

Fazariah et al. made a theoretical study on the electronic structure and magnetic properties of TM (Sc, V, Cr, Mn, Fe, Co, Ni, Cu and Zn)-doped TiO_2 DMS using density functional theory (DFT) (Fazariah et al. 2017). Based on their first-principles calculations it was concluded that both Fe-doped TiO_2 (i.e. TiO_2:Fe) and Mn-doped TiO_2 (i.e. TiO_2:Mn) have large MMs making them good DMS candidates. In this study it was also predicted that TiO_2:Sc and TiO_2:Ni does not show magnetic behavior. Doping of TiO_2 with V, Cr, Co, Cu and Zn also makes it to acquire magnetic properties and thus to become DMS systems. Out of the above DMS systems, TiO_2:Fe emerged the best one having the highest MMs with prospects for the spintronics applications.

However, experiments show that Ni substituted TiO_2 is a good oxide-based DMS candidate to be used in the spintronic devices. Ni^{2+} serves as an efficient dopant in the undoped TiO_2 because of the possible modification in the electrical and magnetic properties. Ni^{2+} substitution for Ti atoms not only provides band-gap tailoring facility but also controls the morphology of the material (Jing et al. 2005). Introduction of oxygen vacancy defects during the synthesis of TiO_2 doped with TM induces magnetic behavior in these materials. Akshay et al. studied the effect of Ni doping in TiO_2 DMS and the substitution of Ti by Ni^{2+} (Akshay et al. 2019). They observed a decrease in the coercivity as a result of Ni substitution. Moreover, in this study lowering of the Ni concentration in TiO_2 resulted in the manifestation of magnetic behavior. This magnetic behavior shown by Ni^{2+} substituted TiO_2 is attributed to the formation of bound magnetic polarons (BMPs) arising due to the oxygen vacancy defects introduced during the synthesis process itself. Band-gap narrowing and enhanced magnetic moment was also observed by the same group for this Ni-doped TiO_2 DMS which makes it a promising material for the development of advanced functional devices in future.

Prajapati et al. investigated the physical properties of Fe-doped TiO_2 DMS NPs (Prajapati et al. 2017). Raman spectroscopy revealed about the structural disfigurement of the lattices as confirmed through a decrease in the intensity and broadening of the characteristic peaks of Fe:TiO_2 compared to the pristine one. Superconducting quantum interference device (SQUID) measurements showed that Fe-doping in TiO_2 causes remnant magnetization (M_r-value) to decrease and the coercivity (H_c-value) to increase. Further, this change in the M_r- or H_c-value was observed to increase with increase in the doping level. The hysteresis shown by the samples corroborate the existence of the weak RTFM in Fe:TiO_2 thereby making it a prospective DMS material.

Undoped TiO_2 NPs prepared through the wet chemical method show FM behavior at RT (Chanda et al. 2018). The origin of this RTFM lies in the intrinsically present oxygen vacancies in the TiO_2. However, in the same study TiO_2:Co NPs (6–8 nm) prepared through the same technique, showed coexistence of FM and PM phases (Fig. 2), but with the enhanced magnetization compared to that for pristine one. This Co doping in TiO_2 resulted into the greater magnetization and the simultaneous existence of PM may be possibly because of the presence of some undetected clusters of oxides of Co. Thus Co doping in TiO_2 is seen as a good choice for changing it into a potential DMS material. Table 1 presents the values of different ferromagnetic parameter at room temperature for bare and TM doped TiO_2 NSs.

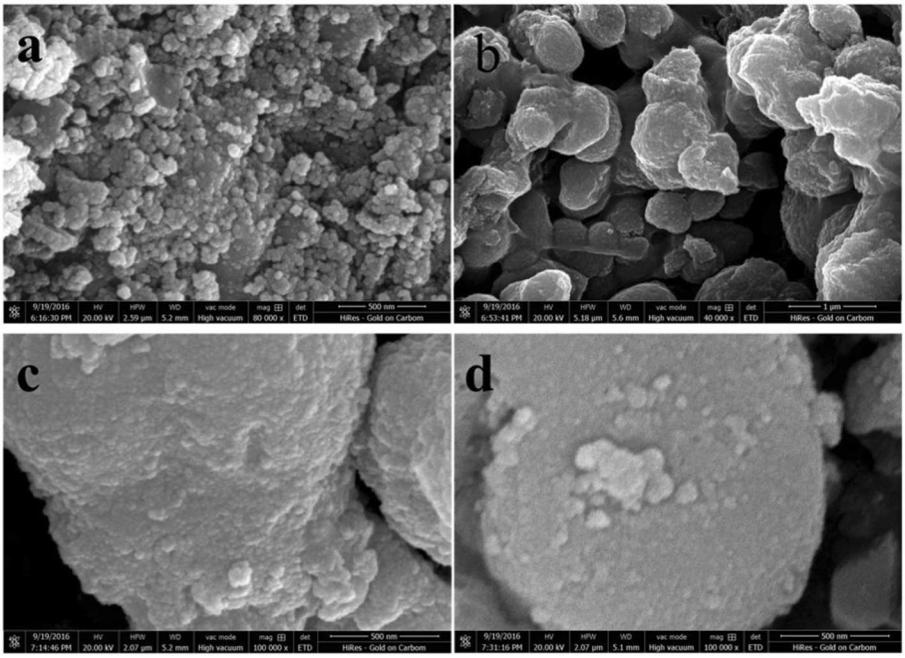

Fig. 2 **a** SEM image of TiO_2 **b** SEM image of 3% Co-TiO_2 **c** SEM image of 5% Co-TiO_2 **d** SEM image of 7% Co-TiO_2 (Chanda et al. 2018)

Table 1 RTFM parameters of bare and TM doped TiO_2 NSs

Dopant	Dopant concentration (%)	Reason for magnetism	Saturation magnetization (M_S)	Coercivity(H_C) Oe	Retentivity or remanence (M_r)	Refs.
Fe	0, 0.1, 0.2	Ti3 + defect, V_O, Fe, BMP	0.109, 0.292, 0.075 emu/g	87,129, 134	0.007, 0.031, 0.008 emu/g	Santara et al. (2014)
Ni	0, 3,6,9,12	BMP, V_O, Ti interstitial defects	$7.21–11.33\times10^{-3}$ μ_B/Ni	~320, 35, 30, 25,10		Akshay et al. (2019)
none	0	Ti^{3+} ions induced V_O	180.4 emu/cc	–	–	Wu et al. (2017)
none	0	Surface oxygen vacancy (V_O), exchange coupling interactions	~0.067 emu/g	–	–	Zhang et al. (2021)
Mn	10,15	Bound magnetic polarons (BMP)	0.035 to 0.017 μ_B/Mn	85, 140		Sharma et al. (2011)
Ni	2, 4, 6, 8	V_O	0.67, 0.92, 1.13 and 1.25 μ_B/Ni	337		Hou et al. (2007a)
Fe	2,8, 5.4	Fe, V_O, other electronic defects	4.7, 4.5 μ_B/Fe			Rodriguez-Torres et al. (2008)
Fe	1, 6, 8, 12	V_O, presence of impurities	0.68, 1.3, 0.15, 0.051 μ_B/Fe			Chen et al. (2006)
Co	3, 5, 7, 10	Charge imbalance, lattice distortion and V_O	0, 1.0, 1.1, 1.5 μ_B/Co	–	–	Fukumura et al. (2008)
Ni	0, 0.5, 1,1.5, 2 and 2.5	F-center induced BMP, oxygen interstitial (I_O) defects	(8.16, 8.04, 6.34, 5.37, 2.4, and 11) $\times10^{-4}$ emu/g	1079, 1405, 1625, 1675, 455, 320	(4.1, 4.4, 4.8, 4.7, 7.9, and 14) $\times10^{-5}$ emu/g	Parveen et al. (2017)

2.1.2 RTFM in ZnO-based DMSs

A prominent DMS system which has greatly attracted the attention of researchers due to its interesting applications is the TM-doped ZnO. This is because of its large band gap energy (3.3 eV) and high excitonic binding energy (60 meV) at RT (Aljawfi and Mollah 2011; Sharma et al. 2004). ZnO shows magnificent chemical stability and exceptional piezoelectric property. ZnO thin films possess several auspicious advantages such as low-priced, copious, high chemical stability, high transparency in the visible and near infrared region, and being safe in use (Jayabharathi et al. 2014). The doping of ZnO with TM introduces greater number of mismatches and defects in its crystal structure. The substitution by magnetic TM ions at the Zn cationic sites in the ZnO host matrix induces FM behavior in these films. Hence, ZnO:TM films are highly suitable for DMS-based device applications. Moreover, ZnO is affable to the environment and is also suitable for the catalytic actions when doped with suitable impurities due to increased surface area (Schmidt-Mende and MacManus-Driscoll 2007).

The doping of ZnO with TM ions of Mn, Co, Ni causes a desirable change in the properties to behave as FM, antiferromagnetic (AFM) or PM (Phan et al. 2012). Some researchers claim that FM in the TM-doped ZnO arises due to the phase segregated impurities (Jayakumar et al. 2007), while others support the view point that it is due to the formation of BMPs among shallow donor-free carriers (Ma and Lou 2011; Wang et al. 2006), and according to some other groups it is due to the Zener's double exchange interaction (Xing et al. 2009b). The better known and the most accepted model to understand RTFM in DMSs is the BMP model which is based upon the conception of indirect interaction between two polarons involving a localized magnetic moment as an interceder.

The magnetic behavior of TM doped ZnO thin films are strongly dependent on the preparation parameters like doping concentration, type of doping elements, and the temperature of the substrates. Oxygen vacancies are found to play a key role in DMSs in general and ZnO in particular. Vijayaprasath et al. developed 3d-TM (0.03 mol %) doped ZnO thin films by the spin-coating sol–gel method (Vijayaprasath et al. 2014). Through their observations, they established that the optical band gap of these films decreases with increasing orbital occupancy by 3d electrons as a reflection of the orbital splitting of magnetic ions. Such thin films exhibited well defined FM characteristics. The surface morphology of these TM-doped ZnO thin films was confirmed through the SEM images. These images indicate that the surface of ZnO films were smooth with small crystallite grain size. The researchers observed a large coercivity and high saturation magnetic moment for TM-doped ZnO thin films which indicate that the RTFM was induced in consequence to the doping with TM ions. Further, it was also observed that the Mn-doped ZnO thin films possess higher saturation magnetic moment as compared to Ni or Co doped ZnO, the possible reason for it being that Mn^{2+} has smaller ionic radius compared to Ni^{2+} or Co^{2+} and also have half-filled 3d electrons.

The incorporation of Mn ions into ZnO nanocrystals leads to a decrease in the band gap energy from 3.23 to 2.63 eV (Alshahrie 2016). Through a novel synthesis of $Zn_{1-x}Mn_xO$ thin films by the 5-methyl-7-methoxyisoflavone modified sol–gel/spin-coating method and characterization with several techniques, it was established that the observed high MMs are possibly due to the creation of surface oxygen vacancies and the role played by the oxidation state of Mn. Further, the replacement of Zn^{2+} by Mn^{2+} ions into the ZnO NSs enhances the number of surface oxygen vacancies. ZnO, because of

its unique properties and electric polarization behavior finds different applications like gas sensors, UV lasers, transparent conductive films, window displays etc. (Wang et al. 2015a).

ZnO thin films doped with Ag (i.e. ZnO:Ag) can be prepared through several methods such as sputtering (Wei et al. 2012), oxidation method (Li et al. 2012), e-beam evaporation technique (Chelouche et al. 2014), and sol–gel method (Kayani et al. 2018). Among different deposition techniques, sol–gel technique has been found to be highly suitable for ZnO film deposition. It is a low-temperature technique to deposit good quality films. Thin films of oxide based semiconductors have been developed with spin-coating method because of the associated advantages such as its simplicity, wider application range and low-temperature formation consisting of small particle size in the films. Doping with silver can transform ZnO from exhibiting (intrinsically) n-type conductivity to acquire more useful p-type conductivity (Shin et al. 2013). The factors in favour of doping of ZnO with Ag are its non-toxic nature, inexpensiveness, high thermal conductivity and excellent electrical conductivity. Doping of ZnO with silver is very promising because of the solubility of silver and its large ionic radius and orbital energy due to the presence of single electron in its outermost orbit (Levard et al. 2011).

Kayani et al. studied the dielectric and magnetic properties of dilute magnetic semiconductors Ag-doped ZnO thin films prepared through low-cost sol–gel dip-coating method at RT to target their spintronic applications (Kayani et al. 2020). The doping concentration of Ag was kept in the range 2–10% by weight. As far as dielectric properties are concerned, these Ag-doped ZnO thin films showed high dielectric constant and tangent loss at low frequencies which decreased with increase in the frequency.They also observed that AC conductivity of these films is small at lower frequencies but is significantly high at higher frequencies. With regard to magnetic properties, the researchers established the occurrence of RTFM in such Ag-doped ZnO thin films due to the formation of BMPs. With increase in the doping concentration, the saturation magnetization decreased and coercivity increased as a result of the cumulative effect of lower crystallite size, creation of BMPs, and the generation of large defects (Fig. 3a). The decrease in the saturation magnetization can be attributed to the non-magnetic behavior of Ag dopants.

Transition metal Cr has gained significant attention of researchers as a dopant in ZnO in the quest of inducing FM properties in it due to the several factors viz. (i) almost equal ionic radii of Cr^{3+} and Zn^{2+} ions leading to easy incorporation of Cr^{3+} into the ZnO host lattice, (ii) Cr itself and all its oxides, except CrO_2, in the ZnO:Cr system being AFM eliminates any role of Cr precipitates in getting factitious FM, and (iii) CrO_2, though being

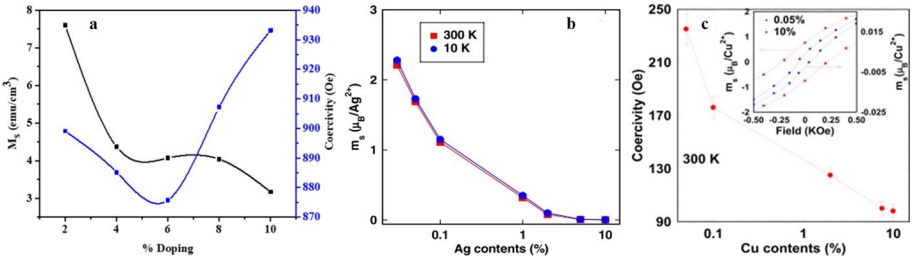

Fig. 3 **a** M_s and H_C versus Ag dopant concentration in ZnO (Kayani et al. 2020), **b** Saturated magnetic moment per Ag^{2+} ion with different Ag contents measured at 300 K and 10 K (Ali et al. 2019a), **c** Dependence of coercivity on Cu-content in ZnO (Ali et al. 2019b)

FM do not form a stable phase and can be easily oxidized to Cr_2O_3 upon heating at atmospheric pressure. Kumar et al. investigated the structural, local-structural and optical properties of sol–gel Cr-doped ZnO (i.e. $Zn_{1-x}Cr_xO$) nanocrystals to thoroughly explore the magnetic behavior of Cr dopants into the ZnO NPs (Kumar et al. 2016). The Cr doping concentration was kept between 0 and 6% (i.e.,$0 \leq x \leq 0.06$). The increasing Cr concentration has an increasing effect in the number of oxygen vacancies as established by the extended X-ray absorption fine structure (EXAFS) study. The FTIR spectra revealed that the local structure around Cr becomes increasingly octahedral with increasing Cr concentration. The increased number of oxygen vacancies with increase in Cr concentration as revealed by FTIR and PL spectra is responsible for distinctive magnetic properties acquired by $Zn_{1-x}Cr_xO$ nanocrystals.

Weak RTFM is also observed in the sol–gel derived ZnO:Co NPs with doping concentration between 0 and 4% (Kumar et al. 2014). The magnetization in the $Zn_{1-x}Co_xO$ NPs increases with increase in the Co doping. In this study, extended X-ray absorption fine structure measurements established that Co doping in ZnO do not appreciably change the host lattice structure, however it leads to the creation of oxygen vacancies. The induction of this (weak) FM is possibly due to the combined effect of grain boundaries, creation of oxygen vacancies and the formation of BMPs. The optical band gap is also affected by Co doping and is found to initially decrease for low values of Co doping and then to increase at higher doping concentrations.

Doping of ZnO with rare earth elements Ho and Sm causes the number of oxygen vacancies to increase which in turn enhances the magnetic properties of ZnO NPs (Ayon et al. 2022). Oxygen vacancies play significant role in mediating the impurity ions leading to the remarkable spin alignment. Thus, TM doping in ZnO has been found to be highly suitable for spintronic applications along with photocatalytic and sensing applications. The RTFM parameters for bare and TM doped ZnO NSs are summarized in Table 2.

Similar to ref. Kumar et al. (2014), the variation in M_s as a function of Ag concentration was also observed by Ali et al. (2019a) as illustrated in Fig. 3b. However, they observed zig-zag variation in H_C with Ag concentration in ZnO. The similar feature of variation of M_s with Cu concentration was observed in another work of Ali et al. (2019b). Here they observed liner variation of H_C in broad range of Cu concentration as demonstrated in Fig. 3c (Table 3).

2.1.3 RTFM in SnO_2-based DMS

Tin Oxide (SnO_2) is an oxygen-deficient n-type semiconductor with a direct wide band gap of about 3.68 eV. It crystallizes in the tetragonal structure and is very useful for solar cell and gas sensor applications because of its high optical transparency, chemical stability and electrical conductivity. Additionally, TM (Fe, Mn, Ni)-doped SnO_2 exhibits RTFM and thus serves as the prospective DMS systems for the development of spintronic devices.

Mn is a good dopant for SnO_2 because it has almost equal ionic radius as that for Sn^{4+} and has large equilibrium solubility. Sol–gel method is the best method for the synthesis of Mn-doped SnO_2 thin films as well as its NSs. Lekshmy et al. studied Mn-doped SnO_2 thin films prepared through the sol–gel dip-coating method and investigated their magnetic properties (Lekshmy et al. 2014). In the quoted study, Mn-doping was kept 0–5 mol%. These films showed PM as well as FM behavior. Magnetization of SnO_2:Mn films strongly depends upon the Mn doping concentration and the M-H curves show the existence of RTFM in these films at higher doping concentration of Mn. The induced magnetic behavior

Table 2 FM parameter of bare and TM doped ZnO NSs observed at RT

Dopant	Dopant concentration (%)	Reason for magnetism	M_S	H_C (Oe)	M_r	Refs.
None	0	Zinc interstitial (I_{Zn})	2×10^{-4} emu/g			Sundaresan et al. (2006a)
None	0	exchange interactions between localized electron spin moments, surface V_o	5×10^{-4} emu/g	~300	~2.1×10^{-4} emu/g	Srinet et al. (2020)
Cr	2, 4, 6, and 8	BMP, oxygen vacancy, Ti interstitial defects, double exchange for ferromagnetic ordering	~2.5 emu/g	64, 72, 78, and 85	7.8, 8.2, 8.7, and 9.2 emu/g	Wang et al. (2014)
Al	1, 3 and 5	V_O	0.0015, 0.005, 0.012, and 0.03 emu/g	70	0.0014 emu/g	Gao et al. (2010a)
Ni	5, 7.5, 10, and 12.5	BMP, V_O	~0.01 emu/g			Rana et al. (2017)
Mn	3	BMP and d^0 ferromagnetism, defects in Zn site	5.5 μ_B/Mn	100		AlmeidaV et al. (2016)
Ni	0.5, 1, 2,3, 5 and 10	V_O	0.0123, 0.0026 emu/g	365, 217	0.002 emu/g	Chithira and John (2018)
Ag	0.03, 0.05, 0.1, 1, 2, 5 and 10	overlapping of BMP, zinc vacancies (V_{Zn})	~2.3, 1.7, 1.1, 0.3, 0.1, 0.03, and 0.01μ_B/Ag	~160, 70, 100, 128, 135, 72 and 128		Ali et al. (2019a)
Cu	0.05, 0.1, 0.5, 1, 2, 2.5, 5, and 10	Cu^{2+} ions mediated by V_{Zn}	1.87, 1.72, 0.38, 0.28 μ_B/Cu and so on	~236, 175, 148, 136, 125, 115, 99, and 93		Ali et al. (2019b)

Table 3 RTFM parameters for TM doped SnO_2 NSs

Dopant	Reason for magnetism	M_S	M_r	H_C (Oe)	Refs.
Sr	Single positive charged V_O,	6.98×10^{-4} emu/g	–	~220	Wang et al. (2015b)
Zn	Single positive charged V_O, Zn atoms in Sn substitutional positions (Zn_{Sn})	0.42 kA/m	0.035 kA/m	700	Delgado et al. (2019)
Ni	free charge carriers and V_o due to the substitution of Ni^{2+} for Sn^{4+}, BMP	0.68 emu/g or 0.298 μ_B/Ni	0.19 emu/g	213	Ahmed et al. (2017)
Cu	Sn vacancies (V_{Sn})	0.2 emu/g	0.019 emu/g	212.90	Chetri and Choudhury (2015)
Co	Co metal clustering, V_O	8.2×10^{-4} emu/g or 0.26 μ_B/Co	–	–	Ali et al. 2015)
Ni	V_O and/or substitution of Ni^{2+} for Sn^{4+}	5.372×10^{-4} emu/g	2.56×10^{-4} emu/g	90	Dorneanu et al. (2016)
Mn	Single positive charged V_O and defects	~4.8×10^{-2} emu/g		~100	Agrahari et al. (2015b)

in SnO_2:Mn films are attributed to the substitution of Mn into SnO_2 lattice. Agrahari et al. investigated the structural, optical and magnetic properties of SnO_2 NPs prepared through the co-precipitation technique at different calcination temperatures and established that even undoped SnO_2 NPs could become magnetic at RT (Agrahari et al. 2015a). The photoluminescence and magnetic properties induced in SnO_2 NPs, so synthesized, are due to the defects and oxygen vacancies created during the synthesis process. The existence of RTFM in these undoped SnO_2 NPs makes it a good DMS candidate. The band gap was observed to show the blue shift at increasing calcination temperature whereas a red shift when compared with bulk SnO_2. F-center exchange coupling is held responsible for the observed increase in the magnetization.

Rai et al. through the first principles calculations using DFT showed that Mo-doped SnO_2 (i.e. $Sn_{1-x}Mo_xO_2$) acquires spin functionality because of the substitution of Sn atoms by the Mo atoms (Rai et al. 2018). It shows a direct band gap and a half-metallic character possessing an integral magnetic moment. Due to the 100% spin polarization, SnO_2:Mo is a prospective DMS material to be used in the spintronic devices. SnO_2 NPs synthesized by the microwave method and doped with TM (Fe, Cd, Cu, Ni, and Zn) showed RTFM as confirmed by the presence of noticeable hysteresis loops (Salah et al. 2017). In this study, SnO_2:Fe NPs showed a wider hysteresis loop signifying for the strong RTFM in it. The FM induced in Fe-doped SnO_2 NPs could be attributed to the presence of defects at the grain boundaries, NPs interfacing sites, oxygen vacancies and existence of dopants. Further, there occurred a slight increase in the energy band gap of some of these samples. Thus SnO_2:Fe could be a good DMS material for the spintronic applications. The induced RTFM in TM-doped SnO_2 is predominantly related to the intrinsic nature of the material itself, especially to the crystal defects and oxygen vacancies created during the synthesis of the material (Fig. 4a–e). The effect of Sr doping on RTFM properties of SnO_2 was systematically studied and found that M_s is nearly linear function of dopant concentration as illustrated in Fig. 4f (Wang et al. 2015b).

2.1.4 RTFM in CuO-based DMS

Copper oxide (CuO) is an AFM oxide semiconductor with narrow band gap ($E_g \sim 1.2eV$) and p-type conductivity. Since, Cu can have three different oxidation states $+1, +2$ & $+3$ and its non-toxic nature, low production cost, and abundance of the materials forming compounds make it a technologically important material. Because of these factors, CuO is being considered as an alternative host material to ZnO for DMS applications. Nanostructured CuO promises a multifunctional nature. It could become a good DMS candidate when suitably doped with some transition metals. The potential applications of CuO include solar cells, gas sensors, catalysis, field emission device, spintronics, energy storage etc. due to its unique properties. Kumar et al. reported the existence of weak ferromagnetism in the sol–gel derived Ni-doped CuO NPs ($Cu_{1-x}Ni_xO$) (Kumar et al. 2021). Rietveld refinement of the XRD spectra and Raman spectra corroborated the single monoclinic DMS phase of $Cu_{1-x}Ni_xO$ with crystallite size between 19 and 21 nm. The energy band gap for these NPs was found to decrease (i.e., red-shifted) from that of pure CuO (1.43 eV). The weak magnetic nature induced in the DMS phase is possibly due to the exchange interaction between the localized magnetic d-spins of dopant ions and the charge carriers from the valence band of pure CuO. The existence of inter-grain magnetic interactions and hence the induction of weak magnetism in this DMS phase is also supported by the quantified value of squareness ratio having a value less than 0.5.

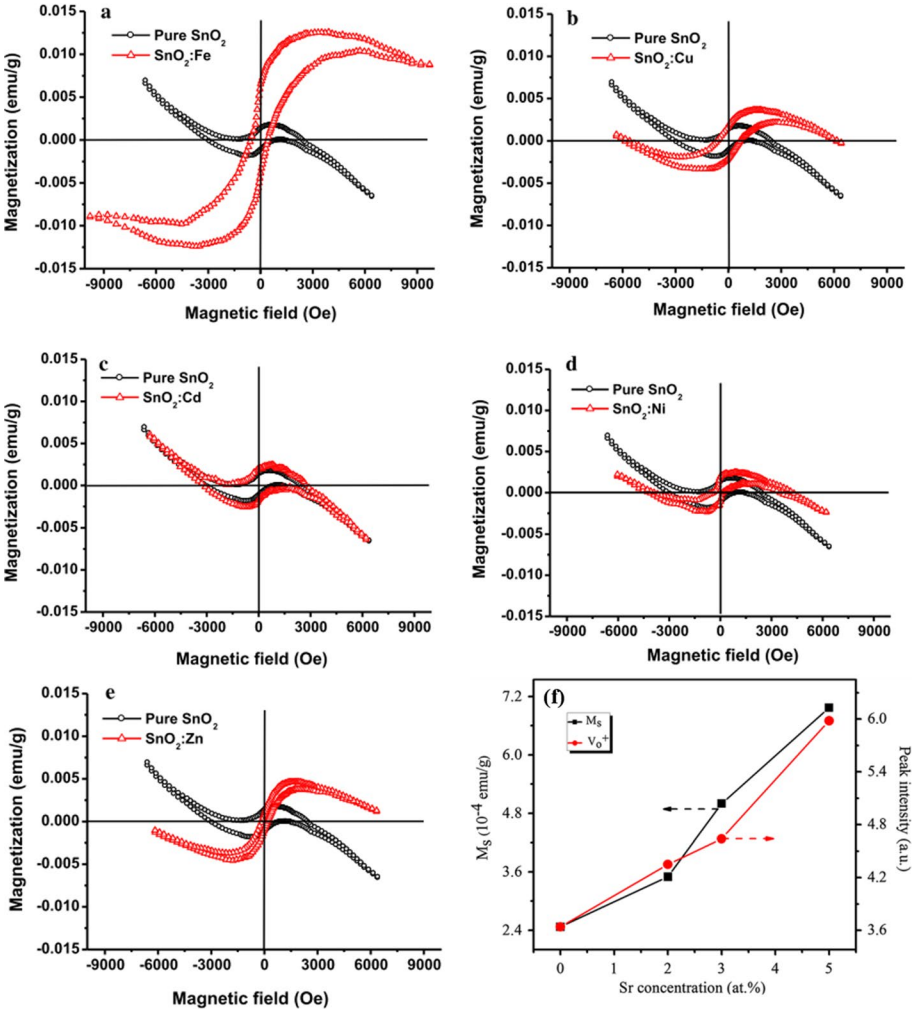

Fig. 4 Room temperature M–H curves of **a**–**e** both bare SnO_2 nanoparticles and doped with different elements at a concentration of 3 mol% (Salah et al. 2017), **f** the saturation magnetization (M_S) and the intensity of the green emission dependent on doping concentration of Sr (Wang et al. 2015b). The values recorded for M_s, M_r, and H_c for TM doped SnO_2 NSs with cause of magnetization are illustrated in Table 3

Ni doping in CuO nanocrystals synthesized through auto-combustion method induces weak RTFM in these crystals (Kamble and Mote 2021). The optical band gap of CuO:Ni nanocrystals increase with increase in the doping concentration of Ni. This increase in the band gap is possibly due to the sp-d exchange interaction between d localized electrons of Ni. The nanocrystalline phase of CuO:Ni was found to be monoclinic and the average crystallite size being 21–24 nm. M-H curves of undoped CuO show ferromagnetic behavior at room temperature even at low fields and are possibly due to the crystallite size. On the other hand the observed RTFM in $Cu_{1-x}Ni_xO$ may be ascribed to the presence of microstrain in the samples. Thus, doping of Ni into CuO makes it a promising DMS material.

Mn-doped CuO nanoflakes synthesized through a simple chemical route showed RTFM, whereas at low temperature of 77 K it shows AFM behavior (Ravi and Shashikanth 2015). In this study, the Mn doping concentration was kept low at 0.5%. The FM/AFM ordering of CuO:Mn could possibly be due to the hopping of Mn^{2+} ions. The existence of high Neel temperature of 99 K makes CuO:Mn a promising DMS candidate for developing future spintronic devices. Dolai et al. studied the effect of incorporation of nanocrystalline Ni into the CuO (i.e. $Cu_{1-x}Ni_xO$) thin films deposited on fused silica substrates by the sol–gel technique (Dolai et al. 2019). The Cu^{2+} substitution by Ni^{2+} ions was confirmed through X-ray photoelectron spectroscopy (XPS) and magnetization of the films was measured by the SQUID. The magnetization was lower at higher temperatures and the ferromagnetic behavior was retained by the films even above the room temperature, hence ensuring CuO:Ni DMS system's suitability for the development of spintronic devices.

2.1.5 RTFM in In_2O_3-based DMSs

Indium oxide (In_2O_3) is a high conductivity, wide direct band gap ($E_g \sim 3.6$ eV) n-type semiconductor at RT. In_2O_3 is optically transparent in the visible spectrum leading to its technological relevance to the wide-ranging optoelectronic applications such as photovoltaic devices, anti-reflective coatings in solar cells, and sensors etc. (Oliveira et al. 2019). It has fascinating prospects for spintronics and magneto-optical applications due to its distinctive electrical, optical, and magnetic properties (especially RTFM) (Yan et al. 2015). TM-doped In_2O_3 DMS films, NPs, nanospheres as well as other morphologies have been widely explored for the existence of FM behavior in them. Single phase and highly oriented rare earth element gadolinium (Gd)-doped In_2O_3 thin films were grown by the pulsed laser technique (PLD) on several substrates (Gupta et al. 2007). These In_2O_3:Gd films for a 10% doping of Gd showed high magnetoresistance ($\sim$ 18%) at a relatively small magnetic field of 1.3 T. TM (Fe, Co, Ni)-doped $In_{2-x}TM_xO_3$ NS thin films were prepared by sol–gel process on substrates such as SiO_2/Si(100), Corning 7059 glass and MgO (100) (In-Bo and Kim 2004). These films showed FM behavior at RT as indicated by the magnetic hysteresis curve and given prospects for their use in the magnetic devices.

The pressure of gaseous environment under which DMS films are deposited affects their magnetic properties. Luo et al. studied the Fe-doped In_2O_3 DMS films deposited under the environment of different oxygen partial pressures (Xi et al. 2018). Fe doping was kept at 5% and oxygen partial pressures of 10^{-3}, 10^{-5}, and 10^{-7} Torr were set for the film deposition. The TEM characterization of these films showed the absence of any clustering or secondary phases for the partial pressures of 10^{-3} and 10^{-5} Torr, whereas increase in the oxygen partial pressure to 10^{-7} Torr leads to the presence of a Fe-rich phase at the interface. It was observed that a decrease in partial pressure leads to an increase in the magnetization of these In_2O_3:Fe DMS films (Fig. 5). The origin of FM in these films is most likely due to the formation of BMPs as indicated by the volume fractions of the FM phases obtained through the muon spin relaxation (μSR) analysis of different samples.

In the doped In_2O_3 system, the FM behavior might be affected by the doping percentage, temperature of the samples, and the site occupancy by the dopant cations. To explore the possible connection between the FM and the above stated factors, Oliveira et al. studied the magnetic behavior and site occupancy in the Fe-doped In_2O_3 i.e. $(In_{1-x}Fe_x)_2O_3$ NPs prepared via a freeze-drying process followed by the heat treatment (Oliveira et al. 2022). Analysis revealed that the iron cations substituted indium cations at both the cationic sites 24d and 8b (though preferably at 8b for low doping

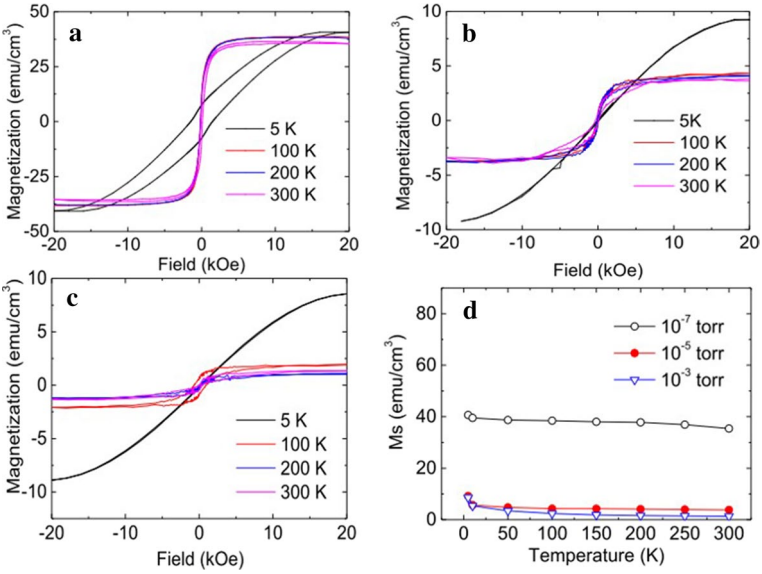

Fig. 5 M-H loops of 5% Fe doped In_2O_3 deposited under **a** $PO_2 = 10^{-7}$ torr. **b** $PO_2 = 10^{-5}$ torr. **c** $PO_2 = 10^{-3}$ torr. **d** Saturation magnetization dependence on temperature of the three samples. (Xi et al. 2018)

concentrations) in the oxide matrix which indicates that the site occupancy is dependent on the value of the doping factor x. Further the magnetic measurements at varied temperatures established the existence of partial FM ordering at RT for the moments at the site 24d whereas for the site 8b it was PM ordering. These In_2O_3:Fe NPs have good prospects to be used as DMS materials for the development of spintronic devices. RTFM was also observed for Ni-doped In_2O_3 NPs prepared by the facile co-precipitation method (Prakash et al. 2011). In_2O_3 samples with different doping concentrations of Ni and characterized with XRD and UV-Vis techniques revealed that the synthesized material consists of a single polycrystalline phase with bixbyite type cubic structure and a significant decrease in the energy band gap occurred for these doped NPs as compared to the pristine one. Further, the DC magnetization measurements established the induction of FM behavior at RT due to the doping of Ni. In_2O_3:Ni samples showed ferromagnetic hysteresis, indicating the presence of RTFM. The magnetization increases with increase in the doping concentration of Ni. However, undoped In_2O_3 also show weak ferromagnetism.

Presence of 3D uniform arrangement of nanospheres and their RTFM behavior in mesoporous DMS may lead to their use in the spintronic nanodevices. Deng et al. synthesized mesoporous 3D nanosphere arrays of $In_{2-x}Co_xO_3$ for several Co concentrations through nanocasting using the mesoporous silica LP-FDU-12 as the hard template (Deng et al. 2015). The observations lead to the monotonically decreasing optical band gap with increasing concentration of Co. The interesting part of the observations was the RTFM behavior superimposed over the PM background for the doped In_2O_3 whereas undoped In_2O_3 showed FM behavior superimposed over the DM background. So doping of Co induces RTFM in In_2O_3 and makes it a fine DMS material with potential to be used for the development of spintronic devices.

2.2 Co-doped DMS systems

The doping of multi ions is found to be an effective way to manipulate the FM behaviors of MOx. It is reported in many cases that co-doping of TM is also used as an effective approach to enhance the RTFM properties of MOx. Yoo et al. (2005) and He et al. (2005) have demonstrated the RTFM in both bulk and thin film Fe and Cu co-doped In_2O_3 samples. In subsequent years Peleckis et al. (2006) and Li et al. (2007) also reported the RTFM in Mn, Fe and Fe, Ni co-doped In_2O_3 respectively. RTFM in In_2O_3 was also observed by co-doping of Fe, Sn ions and the FM properties of the films were attributed to the formation of BMPs due to FM coupling of Fe ions with the electrons trapped by the oxygen vacancies. Further, the long range FM coupling between the BMPs is mediated by the free electrons provided by Sn (Wang et al. 2018). Whereas, the Mn^{2+} vacancy complexes induced magnetic interaction by the overlapping of BMPs were believed to be the cause of RTFM in Mn, Mg co-doped In_2O_3 thin films (Liu et al. 2019). While, the origin of observed RTFM was described based on BMPs model mechanism in Fe, Mn co-doped In_2O_3 nanocubes. In this study theoretical investigations using DFT showed that clusters of impurities (Fe-Mn) robust magnetic interactions within and between the cluster(s). These clusters only contribute FM in systems and thus larger concentration of defects leads to the enhancement in FM (Dhamodaran et al. 2022).

Sakai et al. investigated the magnetic and transport properties of $Fe_xNb_yTi_{1-x-y}O_{2-\delta}$ ($x = 0.06$, $y = 0$, 0.1, 0.03) films deposited by pulsed laser deposition at various partial oxygen pressures (P_{Oxygen}). They observed RTFM only when the partial pressure during deposition kept larger than 1×10^{-6} Torr for all the $Fe_xNb_yTi_{1-x-y}O_{2-\delta}$ films, indicated the requirement of a critical oxygen vacancy density for the FM transition and magnetization increases with increase in concentration of Nb (Sakai et al. 2010). RTFM was recorded for soft-chemical solution processed TiO_2 co-doped with various ^{57}Fe concentrations (0.1–1.0 at.%) and a fixed Sn concentration of 2.0 at.%. It was observed that higher concentration of ^{57}Fe degraded the magnetic properties and oxygen vacancies were believed to be the origin of FM in the systems (Wang et al. 2016). Kumar et al. (2017) studied the influence of Mn and Co co-doping on the RTFM properties of TiO_2 as shown in Fig. 6a and found that M_s and M_r improved by a factor of 1.4 or 2 with respect to Co or Mn doping respectively. The maximum values of M_s and M_r were 14.65×10^{-3} emu/gm and 3.08×10^{-3} emu/gm for $Ti_{0.97}Mn_{0.02}Co_{0.01}O_2$ respectively with H_C value of 212 Oe. A combined approach of first principles and experiments were used

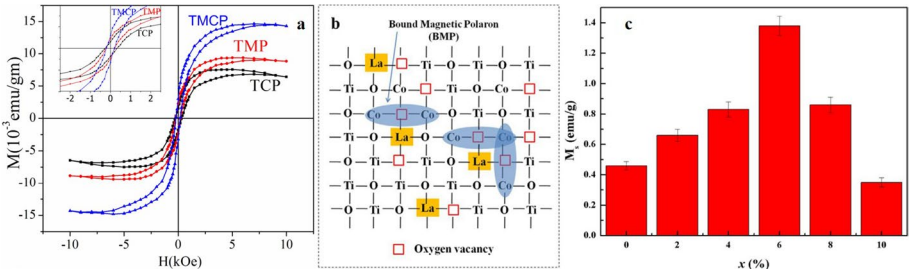

Fig. 6 **a** M-H curves for$Ti_{0.97}Co_{0.03}O_2$(TCP), $Ti_{0.97}Mn_{0.03}O_2$(TMP), and $Ti_{0.97}Mn_{0.02}Co_{0.01}O_2$(TMCP) (Kumar et al. 2017), **b** oxygen vacancies manipulated by La dopant and BMPs yielded through Co^{2+}-□-Co^{2+} ferromagnetic coupling, and **c** La content dependence of saturation magnetization (M_s) (Zhang et al. 2018)

to investigate RTFM of the undoped, N doped, Ru doped, and Ru, N co-doped anatase TiO_2 nanotubes (TNTs) films. The experimental results of the study were lined with the theory calculations and the calculated net moment was in the order of Ru doped > Ru, N co-doped > undoped > N doped with evaluated M_s of 0.065 emu/g, 0.015 emu/g, 0.155 emu/g, and 0.073 emu/g for undoped, N doped, Ru doped, and Ru, N co-doped TiO_2, respectively. They attributed that the hybridization of Ru 4d, N 2p, and O 2p led to the spin-spilt of Ru 4d, N 2p, and O 2p, which is devoted to the system RTFM (Xu et al. 2017). The enhancement in FM properties was also noticed by co-doping of N with Sn in TiO_2 microspheres (Sundaram et al. 2017). The effect of La doping on RTFM of $Ti_{0.97}Co_{0.03}O_2$ was investigated by Zhang et al. (2018). They presented a scheme for manipulation of oxygen vacancies (V_O) by La dopant and BMPs yielded through Co^{2+}-V_O-Co^{2+} ferromagnetic coupling (Fig. 6b). They noticed that M_s increases with increase in La concentration, attains a maximum at 6% of La concentration and then reduces with further increase in dopant concentration (Fig. 6c). The oxygen vacancies were also believed to be the cause of RTFM in Cr, Co co-doped TiO_2 NPs where the value of M_s enhanced with the increase of Cr/Co concentration (Naseem et al. 2019). RTFM in Sr, Co co-doped TiO_2 was attributed to the oxygen vacancies and M_s, M_r and H_c increased with increase in Sr concentration and reached maximum of 2.801 memu/g, 0.27 memu/g and 75 Oe respectively (Rahman et al. 2021).

Co-doping induced tailoring of magnetic properties of ZnO is examined extensively in literature. The observed RTFM parameters in such few systems are summarized in Table 4 and others are discussed here. The observed RTFM in epilayer of $Zn_{1-x-y}Mn_xN_yO$ was attributed to the holes mediated FM ordering of Mn atoms (Liu et al. 2008). Whereas, BMPs models with respect to defect bound carriers was attributed to RTFM in $Zn_{0.95-x}Mn_xLi_{0.05}O$ (x = 0, 0.01, 0.03, 0.05, and 0.08) and MMs/Mn atoms increased with increase in Mn concentration (Zou et al. 2010). The observed RTFM in Co, Al co-doped ZnO NPs calcined at 600°C, increased correspondingly for the calcined particles with Co concentration. Whereas, the sintered compacts of various concentrations of Co and Al dopants showed strong PMs behavior due to grain growth (Siddheswaran et al. 2013). $Fe_xCo_{0.1}Zn_{0.9-x}O$ ($0.0 < x < 0.2$) NPs showed RTFM with small coercivity and M_r whereas M_s and coercivity was increased by Fe doping (Köseoğlu 2015). While the magnetization increased with Mn-doping for Mn, Cu co-doped ZnO NPs (Ashok Kumar and Muthukumaran 2015). The improved values of M_s, M_r, and H_c were recorded by incorporation of Tb ions in Co doped ZnO. They attributed via BMP fitting in their study that the number of BMP is increased in co-doped systems compared to mono doped one and thus enhanced number of BMPs with larger moments is the main reason behind the robust FM (Das et al. 2018). Ali et al. (2019c) also studied the effect of co-doping on RTFM properties of ZnO systematically (Fig. 7a, b). A linear variation in M_s versus H_c is noticed. The mechanism for generation and variation with dopants concentrations are illustrated in Fig. 7c. Magnetization (M) vs. temperature (T) curves of Co, Y co-doped ZnO NPs were recorded under zero field cooled (ZFC) and field cooled (FC) conditions under a magnetic field of 500 Oe (Fig. 7d). The sharp rise of magnetization in the low temperature region and also the separation between FC and ZFC curves from each other in the entire range of temperature signified the presence of FM ordering. They attributed that RTFM is mediated via defects (oxygen vacancy together with surface defects) due to exchange interaction between dopants ions (Bhakta and Chakrabarti 2019). Similar explanation i.e. BMPs caused by a large number of oxygen vacancies in ZnO lattice via incorporation of dopant ions, for the enhancement of FM in Co (fix), Mn (varying) co-doped ZnO was given by Zulfiqar and colleagues. The variation of H_c and H_r as a function of Mn concentration and temperature

Table 4 RTFM parameter for multi-element doped ZnO NSs

Material	M_S (emu/g)	M_r(emu/g)	H_C (Oe)	Refs.
$Zn_{0.95}Mn_0Fe_{0.05}O$	0.09	0.00285	60	Gu et al. (2012a)
$Zn_{0.94}Mn_{0.01}Fe_{0.05}O$	0.14	0.00946	48	
$Zn_{0.90}Mn_{0.05}Fe_{0.05}O$	0.24	0.01124	24	
$Zn_{0.85}Mn_{0.10}Fe_{0.05}O$	0.32	0.01325	30	
$Zn_{0.94}Co_{0.05}Na_{0.01}O$	0.014	0.02	54.5	Gu et al. (2012b)
$Zn_{0.93}Ni_{0.05}Cu_{0.02}O$	0.008	9.25×10^{-4}	45	Tang et al. (2013)
$Zn_{0.92}Ni_{0.05}Cu_{0.03}O$	0.02	1.45×10^{-3}	57	
$Zn_{0.95}Ni_{0.02}Cu_{0.03}O$	0.008	9.37×10^{-4}	74	
$Zn_{0.93}Ni_{0.02}Cu_{0.05}O$	0.003	2.02×10^{-4}	100	
$Zn_{0.98}Ni_{0.01}Fe_{0.01}O$	0.02	0.001	60	Dhiman et al. (2013)
$Zn_{0.96}Ni_{0.01}Fe_{0.03}O$	0.08	0.011	15	
$Zn_{0.94}Ni_{0.01}Fe_{0.05}O$	0.09	0.028	10	
ZnO	0.221	0.0019	91.61	Yakout et al. (2016a)
$Zn_{0.99}Mn_{0.01}O$	0.788	0.108	141.9	
$Zn_{0.99}Co_{0.01}O$	0.514	0.146	452.5	
$Zn_{0.98}Mn_{0.01}Co_{0.01}O$	0.918	0.158	185.6	
$Zn_{0.99-2.5\times0}Nb_0Mn_{0.01}O$	36.4	–	–	Satheesan et al. (2017)
$Zn_{0.99-2.5\times0.005}Nb_{0.005}Mn_{0.01}O$	15.0	–	–	
$Zn_{0.99-2.5\times0.01}Nb_{0.01}Mn_{0.01}O$	17.6	–	–	
$Zn_{0.99-2.5\times0.02}Nb_{0.02}Mn_{0.01}O$	52.0	–	–	
$Zn_{0.99-2.5\times0.03}Nb_{0.03}Mn_{0.01}O$	46.0	–	–	
$Zn_{0.96}Cu_{0.04}Co_{0.0}O$	4.632	0.255	–	Kanwal et al. (2022)
$Zn_{0.94}Cu_{0.04}Co_{0.02}O$	2.014	0.108	–	
$Zn_{0.91}Cu_{0.04}Co_{0.05}O$	1.108	0.057	–	

dependence magnetization noticed by them is illustrated in Fig. 7e, f respectively (Zulfiqar et al. 2021).

The effect of co-doping on RTFM properties of SnO_2 was also investigated (Okabayashi et al. 2012; Xue et al. 2019; Nomura et al. 2011; Mehraj et al. 2015; Vizhi and Rajan 2022; Manikandan and Murugan 2016; Khan and Hu 2015; Khan et al. 2016a, b; Nachiar and Muthukumaran 2019). The Mn, Fe co-doping in SnO_2 enhanced the magnetization in comparison with the case of single-ion doping and saturation magnetization was correlated with the crystalline sizes (Okabayashi et al. 2012). Whereas, M_s increased with increase in Fe concentration in $Sn_{0.97}Sb_{0.03}O_2$ as illustrated in Fig. 8a (Xue et al. 2019). The SnO_2 co-doped systems with one of the dopant of Co are largely explored. Like, Fe (Nomura et al. 2011; Mehraj et al. 2015; Vizhi and Rajan 2022), Zn (Manikandan and Murugan 2016; Khan and Hu 2015; Khan et al. 2016a), Ni (Khan et al. 2016b), and Cu (Nachiar and Muthukumaran 2019) etc. have been doped in Co doped SnO_2. The co-doping of Fe in Co-doped SnO_2 was found to improve FM M_s as compared with SnO_2 doped with only Fe or Co due to the lattice distortion induced by co-doping (Nomura et al. 2011). Similar features were observed in $Sn_{1-x}Fe_{x/2}Co_{x/2}O_2$ ($x=0.04, 0.06, 0.08, 0.1$) NSs where increase in doping concentrations resulted in the structural transformation from NPs to NRs and improved M_s due to generation of large amounts of defects and oxygen vacancies (Mehraj

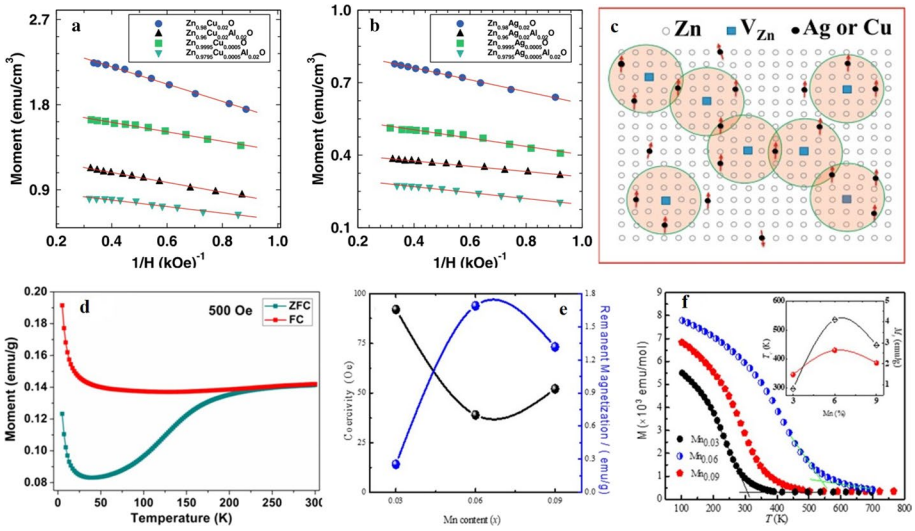

Fig. 7 M-H curves at 300 K for doped and co-doped **a** ZnO:Cu and **b** ZnO:Ag films and **c** Schematic representation of ferromagnetic ordering in ZnO:Cu and ZnO:Ag films mediated through the overlapping of BMPs (Ali et al. 2019c). **d** Magnetization versus temperature curve of Co, Y co-doped ZnO NPs (Bhakta and Chakrabarti 2019). **e** Coercivity, and remnant magnetization as a function of Mn concentration and **f** temperature dependence magnetization (inset shows the remnant magnetization and Curie temperature (T_C) versus Mn content) (Zulfiqar et al. 2021)

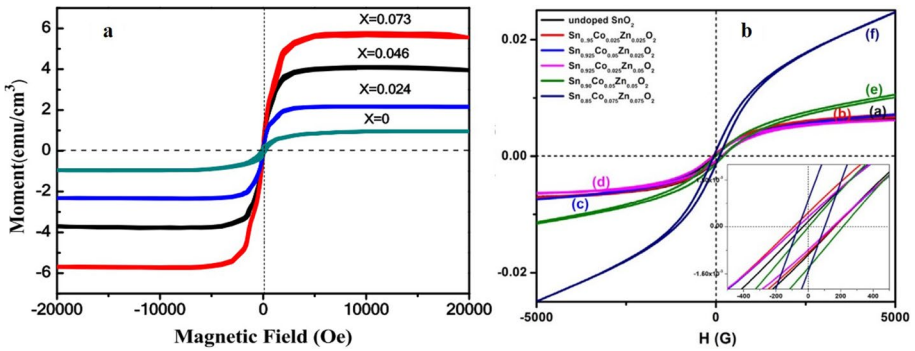

Fig. 8 Room temperature M-H curves of the **a** $Sn_{0.97-x}Sb_{0.03}Fe_xO_2$ films (x = 0.024,0.046 and 0.073) (Xue et al. 2019), **b** with varying concentration of Co and Zn in SnO_2 (Manikandan and Murugan 2016)

et al. 2015). Vizhi et al. also observed an increment in M_s with an increase in Fe concentration whereas the coercivity was reduced. They concluded that the FM properties depend not only on the distribution of defects but also on the surface diffusion of the dopant ions and nanometric size of the materials (Vizhi and Rajan 2022). On the other hand, the less doping of both (2.5% each) Co and Zn in SnO_2 results in highest M_s value. Further increase in concentration of any of the dopant results reduction in M_s value as illustrated in Fig. 8b (Manikandan and Murugan 2016). Khan and colleagues also investigated the effect of Zn in Co doped in SnO_2 on RTFM (Khan and Hu 2015; Khan et al. 2016a). In one of their

study they fix the content of Zn 5% and vary the concentration of Co (1%, 3%, and 5%) (Khan and Hu 2015), whereas in another study they fix Co concentration 3% and vary Zn concentration (1%, 2%, and 3%) (Khan et al. 2016a). Their observations inferred that RTFM induced via Co doping and co-doping of Zn boosted the FM behavior. Similar to Zn, Ni doping also enhanced the FM behavior of Co doped ZnO but upto 2% of Ni doping beyond which FM feature decreased (Khan et al. 2016b). Alike, FM performance were recorded for Cu, Co doped SnO_2 where magnitude of FM increased up to 4% of Co doping and beyond which it was reduced. They attributed RTFM induced via overlapping between BMP by Co-doping and existence of high density charge carriers and oxygen vacancies at 4% of Co might be responsible for highest FM whereas enhanced antiferromagnetic interaction between neighboring Co–Co ions may be the cause of reduction of FM at higher Co concentrations (Nachiar and Muthukumaran 2019).

Yakout et al. (Yakout and El-Sayed 2016b; Yakout 2021a, b) studied the effect of co-doping on the ferromagnetic properties of CuO NSs in a very systematic way. They observed an increase in M_S, M_r and H_c values for the system $Cu_{(1-x-y)}Mn_xCo_yO$ on varying either x or y in between 0 to 2. They assumed the RTFM in bare CuO results from size effect and/or uncompensated Cu^{2+} ions at the surface and the enhancement in RTFM results due to replacement of a non-magnetic Cu^{2+} ion via magnetic TM ions i.e. via Mn^{2+} and Co^{2+} (Yakout and El-Sayed 2016b). The increment in RTFM was also observed by them in another system $Cu_{0.94}Fe_{0.03}M_{0.03}O$ (M = Mn, Co, Ni). They reordered maximum values of FM parameters for the system $Cu_{0.94}Fe_{0.03}M_{0.03}O$. It was noticed that Fe mono-doping helps to boost the RTFM in CuO and superior FM properties may be induced by doping of the binary ions. Remarkably, increase in the M_s and M_r values, by nearly six fold compared to Fe single doping, were recorded especially for Fe/Mn ions. The extra magnetic moment was induced due to substitution of Cu^{2+} via Fe^{3+}, Mn^{2+}, Co^{2+} and Ni^{2+} substitution (Yakout 2021a). Subsequently the same group investigated the effect of Tri-dopants (Mn, Fe, Co) on RTFM properties of CuO NSs. They observed a further improvement in the M_s and M_r values (Yakout 2021b). The comparative results of their studies and the mechanism of RTFM in tri-dopant CuO are shown in Fig. 9 and the parameters observed are summarized in Table 5.

3 Mechanism of RTFM in TM doped MOx

Several experimental (Jing et al. 2005; Akshay et al. 2019; Prajapati et al. 2017; Chanda et al. 2018; Vijayaprasath et al. 2014; Alshahrie 2016; Kumar et al. 2016, 2021, 2017; Lekshmy et al. 2014; In-Bo and Kim 2004; Prakash et al. 2011; Yakout and El-Sayed 2016b; Yakout 2021a, b) as well as theoretical studies (Fazariah et al. 2017; Ali et al. 2019a; Rai et al. 2018; Ahmed et al. 2017; Li et al. 2010; Wang et al. 2007) have been undertaken by researchers so far to understand the mechanism of origin of RTFM in TM doped MOx, but it is still not fully explored and is under debate. As far as theoretical attempts are concerned, four major models have received much acclaim to explain the cause of RTFM in these materials. The first of them, Ruderman-Kittel-Kasuya-Yosida (RKKY) model considering magnetic interaction between individual localized magnetic and delocalized conduction band electrons (Ali et al. 2019b). It is a kind of super exchange interaction between two magnetic ions at nearest or next nearest neighboring positions and is efficacious only in the cases of high concentration of delocalized carriers existing in the host material. The RKKY interaction may lead to both ferromagnetic

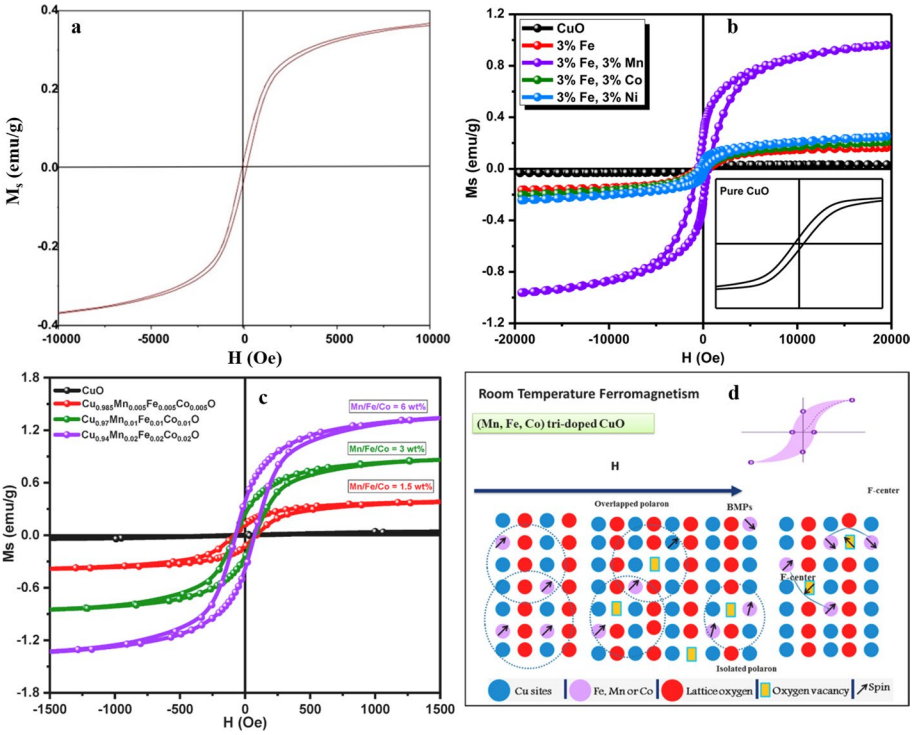

Fig. 9 M–H hysteresis loop of **a** $Cu_{0.96}Mn_{0.02}Co_{0.02}O$ (Yakout and El-Sayed 2016b), **b** pure, Fe doped and Fe/Mn, Co or Ni co-doped CuO nanoparticles (Yakout 2021a), **c** $Cu_{1-3x}Fe_xMn_xCo_xO$ for x = 0, 0.005, 0.01 and 0.02, and **d** Schematics for proposed mechanism of RTFM in $Cu_{1-3x}Fe_xMn_xCo_xO$ (Yakout 2021b)

Table 5 RTFM parameter for Multi-element doped CuO NSs

Material	M_S (emu/g)	M_r(emu/g)	H_C (Oe)	Refs.
CuO	0.107	0.0144	178	Yakout and El-Sayed (2016b)
$Cu_{0.98}Mn_{0.01}Co_{0.01}O$	0.141	0.0080	201	
$Cu_{0.97}Mn_{0.02}Co_{0.01}O$	0.155	0.0030	211	
$Cu_{0.97}Mn_{0.01}Co_{0.02}O$	0.241	0.0190	136.6	
$Cu_{0.96}Mn_{0.02}Co_{0.02}O$	0.370	0.0330	145.4	
CuO	0.031	0.004	183	Yakout (2021a)
$Cu_{0.97}Fe_{0.03}O$	0.163	0.041	570	
$Cu_{0.94}Fe_{0.03}Mn_{0.03}O$	1	0.252	580	
$Cu_{0.94}Fe_{0.03}Co_{0.03}O$	0.209	0.04	240	
$Cu_{0.94}Fe_{0.03}Ni_{0.03}O$	0.293	0.052	250	
CuO	0.032	0.004	183	Yakout (2021b)
$Cu_{0.98.5}Fe_{0.005}Mn_{0.005}Co_{0.005}O$	0.484	0.126	85.4	
$Cu_{0.97}Fe_{0.01}Mn_{0.01}Co_{0.01}O$	1.0025	0.245	75.5	
$Cu_{0.94}Fe_{0.02}Mn_{0.02}Co_{0.02}O$	1.5611	0.389	72.1	

as well as antiferromagnetic alignment of magnetic moments depending upon the separation of interacting atoms. The RKKY interaction mechanism is not responsible for the origin of RTFM in most of the TM doped MOx systems as these have a low density of delocalized carriers.

The Zener model is based upon the concept of magnetic interaction diffusing from one spin to another via indirect exchange interaction mediated by a conduction electron of doped TM ion (Kumar et al. 2021). This kind of FM coupling intermediated by conduction electron may give rise to ferromagnetism but at low temperatures only. Zener model can best explain the origin of ferromagnetism in DMS systems containing TM doping having incomplete *d* shells. The major drawback of this mechanism is that it provides only an approximate quantitative measure of ferromagnetism induced due to exchange interaction among free carriers and localized magnetic moments occurring at critical ferromagnetic temperatures. Zener model is incapable of explaining the cause of RTFM in most of the practical DMS systems.

The mean-field Zener model takes into account the anisotropy of the carrier-mediated exchange interaction alongwith the spin–orbit coupling in the host material followed by the carrier correlation. This mechanism considers the hole-mediated FM interaction between localized spins in a magnetic semiconductor (Xing et al. 2009b). In fact, this model is suitable for explaining long-range interactions combining the effects of spin–orbit coupling and the quantum confinement.

The most acclaimed mechanism for explaining the origin of RTFM in TM doped DMS materials is the bound magnetic polarons (BMPs) model. A BMP is a combination of electrons (or holes) bound to impurity atoms through exchange interactions within an orbit. It considers that the main cause of RTFM in such doped DMS materials is the formation of BMP localized acceptor sites that polarize the TM atoms by the exchange field with the localized holes. The BMP magnetic ordering temperature is dependent on the nature of interactions between charge carriers and atomic spins. The increasing concentration of TM dopants in general causes an increase in the number of surface oxygen vacancies which play a very crucial role in the formation of BMPs (Chanda et al. 2018; Sharma et al. 2011; Ma and Lou 2011; Wang et al. 2006; Alshahrie 2016; Kayani et al. 2020; Kumar et al. 2016; Ayon et al. 2022; Ahmed et al. 2017; Xi et al. 2018; Zhang et al. 2018; Xue et al. 2019).

The ferromagnetism reported in doped MOx may have its origin in intrinsic causes such as defects etc. having basis in the magnetic dopants or due to extrinsic causes such as formation of BMPs through the dopant ion-mediated exchange interaction. To exclude the first possibility and to confirm whether RTFM in ZnO DMS systems is due to extrinsic causes, Nasir Ali et al. studied RTFM in (nonmagnetic) Cu doped ZnO experimentally as well as theoretically (First-principle DFT calculations) (Ali et al. 2019a). It was established through this study that ferromagnetism in ZnO is due to overlapping of BMPs created by exchange interaction of the spin of Cu^{2+} ion with spin of the localized hole due to zinc vacancy (V_{Zn}). Both the theoretical as well as experimental investigations established that the exchange interaction between Cu^{2+}-Cu^{2+} ions mediated by V_{Zn} is responsible for RTFM in Cu-doped ZnO. Stephen J. Pearton et al. studied PLD grown ZnO:Mn thin films (Pearton et al. 2007). They found an inverse correlation between magnetization and electron density which was controlled by Sn doping. The most acceptable mechanism for the origin of ferromagnetic properties in such films is the BMP model or exchange that is mediated by carriers in a spin-split impurity band derived from extended donor orbitals. Such a TM doped ZnO material have been used for the development of polarized solid-state light sources and also highly sensitive biological and chemical sensors.

The electronic or lattice defects present in the materials give rise to intrinsic causes responsible for RTFM in TM doped MOx (Azam et al. 2013; Santara et al. 2014; Akshay et al. 2019; Jayabharathi et al. 2014; Kayani et al. 2020; Agrahari et al. 2015a, 2015b; Salah et al. 2017; Fitzgerald et al. 2006). Majority of studies on TM doped SnO_2 systems indicate that oxygen vacancies and lattice defects are the main factors contributing to ferromagnetic ordering in such DMSs. The doping concentration and sintering temperature have significant effect on RTFM observed in Mn doped SnO_2. The resulting ferromagnetism in such systems may be due to a competing balance between the super-exchange antiferromagnetic coupling and the F-center exchange coupling mechanisms (Ahmad and Mohamed 2012). Studies on Mn doped SnO_2 conclusively established that BMP's overlapping, oxygen vacancies and F-center exchange interaction are the most likely causes for the existence of RTFM in pure and Mn doped SnO_2 system (Ahmad et al. 2018). In Fe doped SnO_2 RTFM has the most likely cause in the formation of BMP's through the V_O created during the synthesis of the material itself. The RTFM observed in Ni doped SnO_2 is mostly reported to be linked to oxygen vacancy and structural defects of the material (Wang et al. 2008). A reduction in the size of the TM doped binary oxides such as TiO_2, ZnO, SnO_2, In_2O_3 etc. can induce FM, even at RT, due to the grain boundary, presence of defects and oxygen vacancies (Gupta et al. 2020).

4 Advantages and drawbacks of TM doped MOx

Metal oxides, being non-toxic in nature are ecologically safe and environment friendly (Fukumura et al. 2004), allow easy doping of transition metals, possess capability of high electron doping and have rather small effective electron mass with better transport properties and making them suitable for realizing high T_C FMs. TM doped MOx i.e., DMS have excellent magnetic and magneto-transport properties and also possess high chemical and mechanical durability (Medhi et al. 2020). Metal oxides are compatible with organic materials which paves way for several applications. MOx nanoparticles are usually prepared through hydrothermal synthesis as this synthesis route brings forth good control over homogeneity, size, morphology, phase, and composition of the synthesized material. TM doped MOx nanoparticles are typically synthesized through the technique of co-precipitation or co-hydrolysis of the precursor of the parent metal with that of the dopant. These materials are suitable for low-cost fabrication of devices. As far as fabrication of spintronic devices is concerned, these materials are advantageous as they allow a simplified device consisting of only an injector and an active semiconducting layer.

Owing the aforementioned advantages, TM doped MOx based DMSs have been successfully transferred into various real time technology products. As DMSs has applications in spintronics that uses the charge and the spin degrees of freedom (ignored in the charge based devices) of electrons simultaneously. This concept has offered designing of devices with advantages of higher speed, greater efficiency, non-volatility, reduced power consumption etc. The discovery of the Giant Magneto-resistive (GMR) structure in 1989 (external magnetic field assisted large change in resistance) was the first ever recognition of the spintronic device. This field is one of the speedily growing field for devices that is transferred from lab to market in the form of read head sensors in hard disc drives. The GMR structures in read heads have been replaced by magnetic tunnel junction (MTJ) devices (exhibited superior performance). Magneto-resistive random access memory (MRAM) is another spintronic device that replaced Si based dynamic random access memory (DRAM).

Besides, being magnetic it is non-volatile, which means not only it retains its memory with the power turned off but also there is no constant power required for frequent refreshing. This can save a significant amount of power for any portable device, which runs under battery. Further, development has shown switching of MMs by spin-polarised currents or spin transfer torque, electric fields, and photonic fields. The field of spintronics can be sub-divided into two broad fields viz. (1) semiconductor and (2) metallic spintronics. Earlier, most of the devices belong to the second class whereas the former one is rich in fundamental science. However, semiconductor spintronics have been realized in many devices such as spin torque oscillator, spin field effect transistors (spin-FETs), race track memories, spin-valve transistors, spin-light emitting diodes (spin-LEDs), non-volatile storage and logic devices etc. (Schmidt and Molenkamp 2001; Heo et al. 2004; Holub and Bhattacharya 2007; Herng et al. 2008; Sharma et al. 2017; Lin et al. 2019; Xue et al. 2020).

In spite of several advantages and success in technological developments as stated above, these materials do face certain challenges which must be taken care of while using them for realizing spintronic devices. DMS have low coercivity which makes it necessary for the application of an external magnetic field for device operation (Prestgard et al. 2014). Moreover, TM doped MOx suffer from the problems of low spin polarization, low dopant solubility, secondary phase separation and bad controllability. Low solubility of dopants results into lesser substitution of host metal by TM and thus results into smaller MMs. Major issues that need improvement are: (i) regulating the uniformity in shape and size of the NSs materials, (ii) inducing significantly high RTFM ordering by controlled doping, (iii) efficient tailoring of the magnetic, electrical, and optical properties, and (iv) formulating a convenient and reproducible method for the development of a series of similar type of DMS materials etc. (Jadhav and Biswas 2016).

In TiO_2, RTFM is mainly due to extrinsic causes such as Co metal precipitations or presence of secondary phases. In some cases, the RTFM has intrinsic origin due to the presence of structural defects such as the oxygen vacancies or interstitials. Synthesis temperature and doping concentration play a significant role in imparting RTFM (mostly by intrinsic means) in TM doped SnO_2 and requires a suitable choice of these parameters for homogeneous and reproducible synthesis of these materials. In the synthesis of TM doped In_2O_3, a careful balance of pressure of gaseous environment is needed for good quality DMS. The local structure and magnetic behavior of TM doped ZnO are very sensitive to the preparation parameters such as temperature, dopant concentration and doping elements (Pan et al. 2008). A precise control over these factors is a challenge for obtaining homogeneously dispersed DMS phase and consequential observation of RTFM in such doped ZnO NSs.

Complementary structural, microstructural, and chemical analyses of various TM doped MOx NSs support hypothetical homogeneous distribution (Nunes et al. 2008) of dopant element in the substitutional sites of the host matrix, but there are cases in which the analysis is suggestive of inhomogeneities in this distribution. DMS of QDs materials faces the problems of phase separation which leads to inhomogeneous distribution of dopant ions (Avijit et al. 2016). However, through suitable choice of synthesis method and preparation parameters, reproducibility of homogeneous DMS phases for spintronic applications can be ascertained.

5 Non-magnetic element doped MOx (RTFM behavior of d^0 materials)

The observation of unexpected FM in undoped HfO_2 thin films by Venkatesan et al. (2004) revived the field of spintronics. Since both, the Hf^{4+} or O^{2-} ions are non-magnetic and the *d* and *f* shells of the Hf^{4+} ion are either empty or completely filled in the above case. Therefore, this FM was intrinsic in nature i.e. induced in the absence of extrinsic magnetic materials and a new term d^0 FM was coined by Coey (2005). Such an unexpected FM was observed in several pure oxides like HfO_2, CaO, ZnO, ZrO_2, TiO_2, MgO, SnO_2 and, even in CaB_6 (Coey 2019; Guillen et al. 2006; M´aca et al. 2008; Singh and Chae 2017; Peng et al. 2009; Ning et al. 2013; Coey 2019) in subsequent years. Consequently, d^0 FM was believed as an alternative of DMSs. The local MMs on the neighboring oxygen atoms induced by point defects such as cation vacancies was whispered of the magnetism in these materials (Ning et al. 2013; Pemmaraju and Sanvito 2005). Alike, TM doped materials suffered with the problem of magnetism reproducibility and homogeneity due to the hitches of defect control. Alternatively, the idea of the substitution of non-magnetic elements (group 1A of periodic table and others) in dioxides such as AO_2 (A = Ti, Zr, or Hf) to tailor d^0 FM via theoretical modelling was put forward by Bouzerar et al. (2006). Following the idea, many ab-initio studies have predicted FM with high Curie Temperature (T_C) in several oxides doped with non-magnetic elements, such as K, Ag and Mg doped SnO_2 (Zhou et al. 2009; Xiao et al. 2011; Guillen et al. 2006), K:ZrO_2 (Zhang and Yan 2009), and Li, K, Mg, and V doped TiO_2 (Tao et al. 2010; Maca et al. 2008; Guuill´en et al. 2008) etc. The d^0 magnetism in non-magnetic elements doped oxides was also observed experimentally in alkali metal, Co and Cu doped ZnO (Chawla et al. 2009a, b; Yi et al. 2010; Ali et al. 2019d; Chouhan et al. 2021a; Dey et al. 2022; Chen et al. 2021); Cu, C Mg, and K doped TiO_2 prepared in thin film form (Hou et al. 2007b; Duhalde et al. 2005; Ye et al. 2009; Srivastava et al. 2011; Chouhan et al. 2021b; Chouhan and Srivastava 2022), K, Li, Ag and Na doped SnO_2 (Chouhan et al. 2021c; Narzary et al. 2022; Srivastava et al. 2010, 2013; Wang et al. 2017), Ag:ZrO_2 (Venkatesan et al. 2004) etc.

Nevertheless, d^0 FM has been reported in various pure and non-magnetic elements doped semiconducting oxides, the observed FM is usually weak in magnitude. In addition, the origin and coupling of MMs in these systems are yet unanswered. However, the common feature in all the investigated systems is the existence of lattice defects. In fact, only a few of the bulk materials showed FM in their pure or defect-free form. In doped systems, FM is originated in some cases due to substitution of non-magnetic ions in cation site and in other cases substitution of non-magnetic ions in anion site whereas in some cases due to cation vacancies and in other cases due to oxygen vacancies. Indeed, the original theory for defect-related FM holds that defects in a semiconductor or insulator produce states in the gap that are abundant enough to generate an impurity band.

The investigations suggested that non-magnetic impurity induced FM either requires the formation of localized states towards the top of the valence band (VB) or just below the conduction band (CB) and electron–electron interaction to flat band. The physics is analogous to the flat band FM. The FM is said to be either caused by MMs associated with molecular orbitals localized at lattice defects or oxygen vacancies mediated exchange interactions between unpaired electron spins at the nano-materials' surfaces (Chouhan et al. 2020).

6 Influence of the morphology on the RTFM

Based on several theoretical as well as experimental studies it has been found that undoped ZnO nanostructures can also exhibit RTFM, which usually shows a morphology dependence (Sundaresan et al. 2006b, Banerjee et al. 2007, Hong et al. 2007). Ren and Xiang have examined systematically and exhaustively morphology-dependent RTFM in quasi-0D, 1D, 2D, and 3D ZnO NSs (Ren and Xiang 20212012). They have concluded on the basis of comparative analysis of the researches like (Wangensteen et al. 2011; Wang et al. 2010; Xu et al. ; Phan et al. 2013) and others that NPs show FM nature for a range of NPs size only and within this range M_s increases with reduction in NPs size. However, FM disappeared beyond both side of that range due to reduction in defect density because of improved crystallinity and recovery of voids within the grains boundary regions for larger particles size whereas for the particles smaller than certain diameter, the cluster formation may reduce the FM feature. In case of NWs/NTs array RTFM was found height and morphology dependent. Magnetization increased with increase in height of the NWs and ascribed to a higher number of Zn–S bond spins formed at the ZnO-thiol interface. Similarly, the NTs exhibited a higher M_s than the NWs due to its larger surface-to-volume ratio and thus higher density of Zn–S bond spins (Deng et al. 2010). Contrary, the change of diameter has no obvious effect on RTFM. Whereas, in case of NRs RTFM reduces with increase in length of the rods due to increased concentration of the V_O and V_{Zn}^{-} and decreased the Zn_i (Yan et al. 2008). Ren and Xiang (2021) have illustrated a bar-diagram to summarize the effect of morphology on RTFM on various ZnO NSs (Fig. 10). Here, ZnO horizontal NWA has the highest M_s.

Kim et al. (2016) developed rice-like and rod-like ZnO NSs. They observed a dramatic enhancement in M_s at the point where the morphology of rice-like ZnO turns into rod-like ZnO. The enhancement in magnetization due to change in morphology was found to be partly due to increase in oxygen vacancy and partly because of increase in surface-to-volume ratio in rod-like nanostructures. Whereas, Motaung et al. (2014) investigated the influence of various hexagonal shapes like nanorods, nanocups, nanosamoosas, nanoplatelets, and hierarchical nano "flower-like" structures on RTFM. They observed enhanced RTFM parameters for the hierarchical flowers and samoosas as compared to their counterparts, platelet- and "cup-like" structures as summarized in Table 6.This was consistent with the

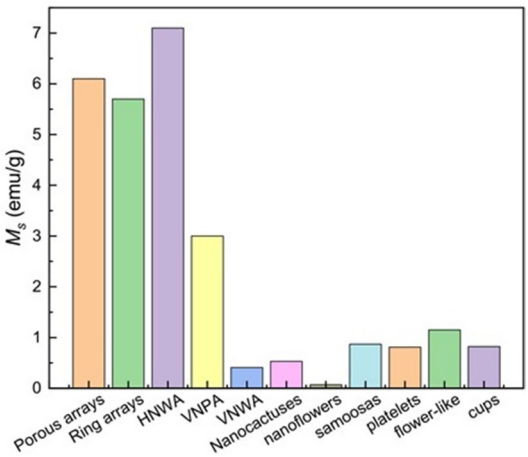

Fig. 10 Saturation magnetizations (M_s) of various ZnO nanostructures (Hong et al. 2007)

Table 6 Coercive Fields (H_c), Remanent Magnetizations (M_r), and Saturation Magnetizations (M_s) of Various ZnO NSs

Nanostructures	Hc (Oe) ± 5.0	Mr ($\times 10^{-4}$) (emu/g) ± 0.01	Ms (emu/g) ± 0.06	μ (μ_b) ± 0.0005
Samoosa	197.42	2.17	0.87	0.0127
Platelets	115.06	1.55	0.81	0.0118
Hierarchical flower	213.62	7.77	1.15	0.0168
Cups	189.58	1.46	0.82	0.0120

EPR and PL analyses which revealed that both hierarchical flowers and samoosas contain more V_{Zn} andV_O^+.

The shape of the nanorods was changed from hexagon (L ~ 1.5 μm, D ~ 200 nm) to pencil like tip (L ~ 1 μm, D ~ 80 nm) with increase in M_s by increasing Ni content from 1 to 3% in ZnO. Further, the observed RTFM and change in magnetism was considered to be mainly due to the coexistence of the magnetic dopants (Ni) and morphological changes (Ahmed et al. 2012). Indeed, it was noticed that 1D TiO_2 NSs such as NWs and NBs exhibited prominent intrinsic FM as compared to thin films due to greater number of surface defects. Undoped and Ni-doped TiO_2 NWs were synthesized through solvothermal process (Hoa and Hiyen 2013) and NRs array synthesized through hydrothermal method (Al-Jawad et al. 2021) and were examined for RTFM by means of several characterization techniques. Firstly, it was established that an increase in doping concentration in both doped NWs & NRs increases M_r and M_S possibly due to enhanced FM coupling between Ni^{2+} ions via F^+ center in the former case and due to exchange interaction between free delocalized carriers (holes from valence band) and the localized d spins of Ni ions in the latter case. In case of Ni-doped TiO_2 NPs the M_S of doped sample was lower than the undoped one and Ms decreased first up to 10% Ni concentration and then increased (Manzoor et al. 2018). Whereas in other report M_s decreased with increase in doping concentration of both Ni and Fe (Hong et al. 2004).

Manna et al. recorded enhanced magnetic properties in Fe-doped CuO NR with increased concentration of Fe due to increase in FM coupling interaction. They attributed the shape anisotropy as the key for improved magnetic behaviour. The shape anisotropy basically resulted in superior magnetic properties in NRs as compared to other morphologies such as thin films or NPs (Manna and De 2010). Some other studies on CuO established that surface morphology of a material is able to modulate RTFM as a result of different surface areas (Gao et al. 2010b; Meneses et al. 2008). Besides, different morphologies of undoped/ TM-doped In_2O_3 and SnO_2 NSs have also been shown to affect RTFM in these materials and the acquired knowledge about the change in their magnetic characteristics is very useful for the selection of suitable morphology of a particular DMS material for the development of spintronic devices. Ahmed et al. (2016) studied the effect of morphology on various properties of DMS. They observed that morphology varies from NPs- NSs-NRs with crystalline structure variation from cubic-mixed-hexagonal. Their recorded minimum and maximum M_s values for NSs and NRs and attributed the change in Ms value to the change in electronic structures that associated with change in shape of nanostructures, which exhibits difference in the bond structures between a center ion and its nearest cations, leads high defect formation energy that contributes the FM.

7 RTFM in 2D MOx

An extensive research interest has been paid off on various 2D materials including MOx after the discovery of graphene to realize novel functionalization and applications. The physical and chemical properties of MOx monolayers along with structures are very different from their bulk counterparts due to reduced bonding coordination and strong surface polarization. These 2D MOx have shown potential applications in supercapacitors, batteries, photocatalysis, gas and bio-sensing, spintronics etc. (Yang et al. 2019). In particular, the discovery of magnetic 2D materials offers endless opportunities for applications in quantum computation, spintronics, data storage, and other memory devices (Cortie et al. 2020; Song et al. 2018). Schmidt et al. probably first, demonstrated FM coupling in Co doped graphene-like (graphitic) ZnO sheet using first-principles calculations. Their results showed that the magnetism is ruled by the topology, namely, the substitutional Co atoms are embedded in a 2D ZnO sheet and a direct exchange interaction induced magnetism in these sheets, which is different from the superexchange interaction in bulk 3D ZnO stacking (Schmidt et al. 2010). Another interesting DFT prediction demonstrated PM to FM phase transition in hole doped 2D (monolayer) SnO for hole density typically above 5×10^{13} cm^{-2}. First-principle simulations inferred that Sn vacancies and Sn vacancy-hydrogen complexes are found to act as shallow acceptors, with equivalently low formation energies in 2D SnO under O-rich conditions. The FM ordering is stabilized due to spin-polarized gap states near the valence band-edge offered by these defects (Houssa et al. 2018).

Experimentally, Yadav and coworkers (Yadav et al. 2018) demonstrated the synthesis of a new 2D oxide magnetic material (Chromiteen) from natural ore via sonication-assisted liquid-phase exfoliation just after the synthesis of non-van der Waals magnetic "hematene" (2D α-Fe_2O_3) (Balan et al. 2018). The FM nature in chromiteen with $M_s \sim 40$ times larger than in chromite was induced via joint effect of vacancies and Cr termination in chromiteen as confirmed by DFT calculations. In subsequent year, Kvashnin et al. (2019) theoretically and experimentally investigated 2D CuO in a bilayer graphene matrix. However, the AFM suggested that the rectangular atomic structure in the ground state of 2D CuO was found to be favorable state. DFT and Universal Structure Predictor: Evolutionary Xtallography (USPEX) methods were performed to calculate high temperature stability of up to 600 K by 2D CuO and to reveal FM and AFM spin ordering. In the same year, Bandyopadhyay et al. (2019) investigated and explained the nature of magnetic ordering in non-Van der Waals 2D chromia (α-Cr_2O_3) and showed that FM ground state resulted because of larger inter-transition metal distances and suppressed AFM super exchange. Further, the magnetic ordering can be tuned by modulating the band gaps. Whereas, Yin and co-workers (Yin et al. 2019) reported that immense vacancy concentration produces strong RTFM with M_s of 50.9 emu/g in 2D ZnO nanosheets. The observed value of M_s was an order of magnitude higher than other ZnO nanostructures and comparable to the conventional FM Fe_3O_4. Further, they showed via the DFT calculations that large concentrations of V_{Zn} can form spontaneously during synthesis when stabilized by H ions, and grain boundaries facilitated further formation of V_{Zn}. For the induction of FM removal of the H ion is essential. Recently, Wang et al. (2021) introduced an atomic chemical-solution strategy to grow wafer-size NiO thin films with controllable thickness down to sub-nanometer scale (0.92 nm) and showed that the magnetic symmetry of NiO broken due to surface lattice defects and resulted in surface FM behaviors. Their sub-nanometric NiO thin film exhibited the highest reported RTFM behavior with a M_s and H_c of 157 emu/cc and 418 Oe respectively. Whereas Chen et al. (2021) observed transitions between PM, FM and less ordered phases due to the interplay between impurity-band-exchange and

superexchange interactions in graphitic ZnO by varying the Co doping level. Their study opens another path to 2D RTFM with the advantage of exceptional tunability and robustness. Kumbhakar et al. (2021) reviewed emerging 2D MOx and summarized their applications. Their study particularly illustrated a thorough and systematic summary of research carried out on layered 2D oxides both from an experimental and theoretical perspective. They discussed several different classes of MOx in their 2D forms such as MOx, MOx_p, M_pOx_q (where M stands for metals; p and q are possible oxidation states)".

8 Conclusions

A brief overview on the existence of RTFM behavior in the bare, magnetic, and non-magnetic elements doped MOx-based is presented here. Though, the MOx systems have been under exploration for more than two decades, these systems still continue to attract great attention of material scientists to achieve new dimensions in the RTFM properties. The origin of FM in different DMS materials has been discussed using various models like Ruderman-Kittel-Kasuya-Yosida (RKKY), Zener, mean-field Zener, and bound magnetic polarons (BMPs) etc. In many cases, FM may be induced either due to the intrinsic causes like surface V_o and V_o or the extrinsic ones I_{TM}. Presence of defects and V_o created during the synthesis of the materials and the formation of BMPs are the most likely causes for the enhanced FM behaviour in DMSs. Ni^{2+} serves as an excellent dopant in TiO_2 and exhibits V_O induced RTFM. For most of the other dopants too, presence of oxygen vacancies provides the base for inducing RTFM in TiO_2, ZnO, CuO, SnO_2 and In_2O_3 DMSs. Formation of V_O-mediated BMPs is the most acceptable mechanism for explaining the origin of RTFM in DMS systems. Ionic radius of dopants also plays a crucial role in determining the induced saturation magnetic moments and shows an inverse relationship between these two. The co-doping strategy and morphology affecting the FM behavior of the materials is also discussed here. TM-doped ZnO is the most extensively studied of all the MOx-based DMSs due to being environment-friendly, low priced and the availability of facile synthesis techniques besides possessing high chemical stability and high transparency in the visible and infrared regions. In spite of various advantages and technology transfer in daily life, DMSs suffer with certain drawbacks. To overcome these limitation of DMSs, researcher are extensively exploring d^0 (non-magnetic doped) and *2D* MOx materials.

Author contributions SS and PK conceived the idea and edited the manuscript. SS and ZHK contributed in writing the introduction section. ZHK and VK wrote section on ZnO. SS and NS wrote section on TiO_2. SS and PK wrote the section on influence of the morphology and advantages and drawbacks of TM doped MOx. SS wrote the section on mechanism of RTFM in TM doped MOx. ST wrote section on CuO. NS wrote the section on In_2O_3, 2D MOx, contributed in tables, figures and editing of manuscript. PK wrote the section on SnO_2, Co-doped DMS systems, d^0 materials, and made the tables and figures.

Funding None of the author received fund from any source for this work.

Availability of data and materials This declaration is "not applicable".

Declarations

Competing interests There is no competing interests of a financial or personal nature.

Ethical approval This declaration is "not applicable".

References

Agrahari, V., Mathpal, M.C., Kumar, M., Agrawal, A.: Investigations of optoelelectronic properties in DMS SnO_2 nanoparticles, Journal of Alloys and Compounds. J. Alloys Compd **622**, 48 (2015a). https://doi.org/10.1016/j.jallcom.2014.10.009

Agrahari, V., Tripathi, A.K., Mathpal, M.C., Pandey, A.C., Mishra, S.K., Shukla, R.K., et al.: Effect of Mn doping on structural, optical and magnetic properties of SnO_2 nanoparticles. J. Mater. Sci. Mater. Electron. **26**, 9571 (2015b). https://doi.org/10.1007/s10854-015-3620-0

Ahmad, S.A., Mohamed, S.H.: Room temperature ferromagnetism behavior of $Sn_{1-x}Mn_xO_2$ powders. J. Magnet. Magn. Mater. **324**, 812 (2012). https://doi.org/10.1016/j.jmmm.2011.09.025

Ahmad, N., Khan, S., Mohsin, M., Ansari, N.: Optical, dielectric and magnetic properties of Mn doped SnO2 diluted magnetic semiconductors. Ceram. Intern. **44**, 15972 (2018). https://doi.org/10.1016/j.ceramint.2018.06.024

Ahmed, S.A.: Structural, optical and magnetic properties of Mn-doped ZnO samples. Results Phys. **7**, 604–610 (2017). https://doi.org/10.1016/j.rinp.2017.01.018

Ahmed, F., Arshi, N., Anwar, M.S., Lee, S.H., Byon, E.S., Lyu, N.J., et al.: Effect of Ni substitution on structural, morphological and magnetic properties of $Zn_{1-x}Ni_xO$ nanorods. Current Appl. Phys. **12**, S174 (2012). https://doi.org/10.1016/j.cap.2012.02.054

Ahmed, B., Kumar, S., Kumar, S., Ojha, A.K.: Shape induced (spherical, sheets and rods) optical and magnetic properties of CdS nanostructures with enhanced photocatalytic activity for photodegradation of methylene blue dye under ultra-violet irradiation. J. Alloys Compd. **679**, 324 (2016). https://doi.org/10.1016/j.jallcom.2016.03.295

Ahmed, A., Ali, T., Siddique, M.N., Ahmad, A., Tripathi, P.: Enhanced room temperature ferromagnetism in Ni doped SnO_2 nanoparticles: a comprehensive study. J. Appl. Phys. **122**, 083906 (2017). https://doi.org/10.1063/1.4999830

Akshay, V.R., Arun, B., Mandal, G., Vasundhara, M.: Structural, optical and magnetic behaviour of sol-gel derived Ni-doped dilute magnetic semiconductor TiO_2 nanocrystals for advanced functional applications. Phys. Chem. Chem. Phys. **21**, 2519 (2019). https://doi.org/10.1039/C8CP06875E

Alam, M., Mandal, K.: Room temperature ferromagnetism and ferroelectricity in double perovskite Y_2NiMnO_6 thin film. J. Magn. Magn. Mater. **512**, 167062 (2020). https://doi.org/10.1016/j.jmmm.2020.167062

Ali, A., Sarfraz, A.K., Ali, K., Mumtaz, A.: Structural, optical, Induced ferromagnetism and anti-ferromagnetismin SnO_2 nanoparticles by varying cobalt concentration. J. Magnet. Mag. Mater. **391**, 161 (2015). https://doi.org/10.1016/j.jmmm.2015.04.106

Ali, N., Vijaya, A.R., Khan, Z.A., Tarafder, K., Kumar, A., Wadhwa, M.K., et al.: Ferromagnetism from non-magnetic ions: Ag-doped ZnO. Sci. Rep. **9**, 20039 (2019a). https://doi.org/10.1038/s41598-019-56568-8

Ali, N., Singh, B., Khan, Z.A., Vijaya, A.R., Tarafder, K., Ghosh, S.: Origin of ferromagnetism in Cu-doped ZnO. Sci. Rep. **9**, 2461 (2019b). https://doi.org/10.1038/s41598-019-39660-x

Ali, N., Singh, B., Ghosh, S.: Room temperature ferromagnetism in ZnO: Cu and ZnO: Ag co-doped with Al. J. Magnet. Mag. Mat. **492**, 165618 (2019c). https://doi.org/10.1016/j.jmmm.2019.165618

Ali, N., Singh, B., Khan, Z.A., Vijaya, A.R., Tarafder, K., Ghosh, S.: Origin of ferromagnetism in Cu-doped ZnO. Sci. Rep. **9**, 2461 (2019d). https://doi.org/10.1038/s41598-019-39660-x

Al-Jawad, S.M.H., Ismail, M.M., Gazi, S.F.: Characteristics of Ni-doped TiO_2 nanorod array films. J. Austral. Ceram. Soc. **57**, 295 (2021). https://doi.org/10.1007/s41779-020-00530-9

Aljawfi, R.N., Mollah, S.: Properties of Co/Ni codoped ZnO based nanocrystalline DMS. J. Magn. Magn. Mater. **323**, 3126 (2011). https://doi.org/10.1016/j.jmmm.2011.06.069

Alshahrie, A.: Synthesis and characterization of dilute magnetic semiconductor based on $Zn_{1-x}Mn_xO$ thin films prepared by 5-methyl-7-methoxyisoflavone modified sol-gel/spin-coating technique. Mater. Res. Bull. **84**, 382 (2016). https://doi.org/10.1016/j.materresbull.2016.08.047

Ashokkumar, M., Muthukumaran, S.: Enhanced room temperature ferromagnetism and photoluminescence behavior of Cu-doped ZnO co-doped with Mn. Phys. E **69**, 354 (2015). https://doi.org/10.1016/j.physe.2015.02.010

Avijit, S., Amitha, S., Pavan, A.R., Soma, C., Tomohiro, S., Ranjani, V.: Uniform doping in quantum-dots-based dilute magnetic semiconductor. Phys. Chem. Lett. **7**, 2420 (2016). https://doi.org/10.1021/acs.jpclett.6b01099

Ayon, S.A., Jamal, M., Billah, Md.M., Neaz, S.: Augmentation of magnetic properties and antimicrobial activities of band gap modified Ho^{3+} and Sm^{3+} doped ZnO nanoparticles: a comparative experimental study. J. Alloys Compd. **879**, 163179 (2022). https://doi.org/10.1016/j.jallcom.2021.163179

Azam, A., Ahmed, F., Habib, S.S., Khan, Z.H., Salah, N.A.: Fabrication of Co-doped ZnO nanorods for spintronic devices. Met. Mater. Int. **19**, 845 (2013). https://doi.org/10.1007/s12540-013-4027-1

Balan, A.P., Radhakrishnan, S., Woellner, C.F., Sinha, S.K., Deng, L., De Los, R.C., et al.: Exfoliation of a non-van der Waals material from iron ore hematite. Nat. Nanotechnol. **13**, 602 (2018). https://doi.org/10.1038/s41565-018-0134-y

Bandyopadhyay, A., Nathan, C.F., Jariwala, D., Shenoy, V.B.: Engineering magnetic phases in two-dimensional non-van der waals transition-metal oxides. Nano Lett. **19**, 7793 (2019). https://doi.org/10.1021/acs.nanolett.9b02801

Banerjee, S., Mandal, M., Gayathri, N., Sardar, M.: Enhancement of ferromagnetism upon thermal annealing in pure ZnO. Appl. Phys. Lett. **91**, 182501 (2007). https://doi.org/10.1063/1.2804081

Bhakta, N., Chakrabarti, P.K.: Defect induced room temperature ferromagnetism and optical properties of (Co, Y) co-doped ZnO nanoparticles. J. Magnet. Magn. Mater. **485**, 419 (2019). https://doi.org/10.1016/j.jmmm.2019.03.106

Bhandarkar, L.V.: Structural and magnetic behavior of Mn doped ZnO synthesized by soft chemical route. Int. J. Innov. Res. Sci. Eng. Technol. **3**, 17150–17153 (2014). https://doi.org/10.15680/IJIRSET.2014.0311008

Boscherini, F.: X-ray absorption fine structure in the study of semiconductor heterostructures and nanostructures. In: Lamberti, C. (ed.) Characterization of Semiconductor Heterostructures and Nanostructures, p. 289. Elsevier, Amsterdam (2008)

Bououdina, M., Omri, K., El-Hilo, M., El Amiri, A., Lemine, O.M., Alyamani, A., et al.: Structural and magnetic properties of Mn-doped ZnO nanocrystals. Phys. E **56**, 107 112 (2014). https://doi.org/10.1016/j.physe.2013.08.024

Bouzerar, G., Ziman, T.: Model for vacancy-induced d^0 ferromagnetism in oxide compounds. Phys. Rev. Lett. **96**, 207602 (2006). https://doi.org/10.1103/PhysRevLett.96.207602

Cao, Q., Yan, S.: The predicaments and expectations in development of magnetic semiconductors. J. Semicond. **40**, 081501 (2019). https://doi.org/10.1088/1674-4926/40/8/081501

Chanda, A., Rout, K., Vasundhara, M., Joshi, S.R., Singh, J.: Structural and magnetic study of undoped and cobalt doped TiO_2 nanoparticles. RSC Adv. **8**, 10939 (2018). https://doi.org/10.1039/c8ra00626a

Chawla, S., Jayanthi, K., Kotnala, R.K.: Room-temperature ferromagnetism in Li-doped p-type luminescent ZnO nanorods. Phys. Rev. B **79**, 125204 (2009a). https://doi.org/10.1103/physrevb.79.125204

Chawla, S., Jayanthi, K., Kotnala, R.K.: High temperature carrier controlled ferromagnetism in alkali doped ZnO nanorods. J. Appl. Phys. **106**, 113923 (2009b). https://doi.org/10.1063/1.3261722

Chelouche, A., Djouadi, D., Merzouk, H., Aksas, A.: Influence of Ag doping on structural and optical properties of ZnO thin films. Appl. Phys. A **115**, 613 (2014). https://doi.org/10.1007/s00339-013-8029-0

Chen, J., Rulis, P., Ouyang, L., Satpathy, S., Ching, W.Y.: Vacancy enhanced ferromagnetism in Fe-doped rutile TiO_2. Phys. Rev. B **74**, 235207 (2006). https://doi.org/10.1103/PhysRevB.74.235207

Chen, R., Luo, F., Liu, Y., Song, Y., Dong, Y., Wu, S.: Tunable room-temperature ferromagnetism in co-doped two-dimensional van der waals ZnO. Nat. Comm. **12**, 3952 (2021). https://doi.org/10.1038/s41467-021-24247-w

Chetri, P., Choudhury, A.: Investigation of structural and magnetic properties of nanoscale Cu doped SnO_2: an experimental and density functional study. J. Alloys Comp. **627**, 261 (2015). https://doi.org/10.1016/j.jallcom.2014.11.204

Chithira, P.R., John, T.T.: Defect and dopant induced room temperature ferromagnetism in Ni doped ZnO nanoparticles. J. Alloys Comp. **766**, 572 (2018). https://doi.org/10.1016/j.jallcom.2018.06.336

Chouhan, L., Srivastava, S.K.: Observation of room temperature d^0 ferromagnetism, band-gap widening, zero dielectric loss and conductivity enhancement in Mg doped TiO_2 (rutile + anatase) compounds for spintronics applications. J. Solid State Chem. **307**, 122828 (2022). https://doi.org/10.1016/j.jssc.2021.122828

Chouhan, L., Bouzerar, G., Srivastava, S.K.: d^0 Ferromagnetism in Ag-doped monoclinic ZrO2 compounds. Vacuum **182**, 109716 (2020). https://doi.org/10.1016/j.vacuum.2020.109716

Chouhan, L., Bouzerar, G., Srivastava, S.K.: d0 ferromagnetism in Li-doped ZnO compounds. J. Mater. Sci. Mater. Electron. **32**, 6389 (2021a). https://doi.org/10.1007/s10854-021-05355-1

Chouhan, L., Bouzerar, G., Srivastava, S.K.: Effect of Mg-doping in tailoring d^0 ferromagnetism of rutile TiO_2 compounds for spintronics application. J. Mater. Sci. Mater. Electron. **32**, 11193 (2021b). https://doi.org/10.1007/s10854-021-05784-y

Chouhan, L., Panda, S.K., Bhattacharjee, S., Das, B., Mondal, A., Parida, B.N.: Room temperature d^0 ferromagnetism, zero dielectric loss and ac-conductivity enhancement in p-type Ag-doped SnO_2 compounds. J. Alloys Comp. **870**, 159515 (2021c). https://doi.org/10.1016/j.jallcom.2021.159515

Coey, J.M.D.: d^0 ferromagnetism. Solid State Sci. **7**, 660–667 (2005). https://doi.org/10.1016/j.solidstatesciences.2004.11.012

Coey, J.M.: Magnetism in d^0 oxides. Nat Mater. **18**, 652–656 (2019). https://doi.org/10.1038/s41563-019-0365-9

Cortie, D.L., Causer, G.L., Rule, K.C., Fritzsche, H., Kreuzpaintner, W., Klose, F.: Two-dimensional magnets: forgotten history and recent progress towards spintronic applications. Adv. Funct. Mater. **30**, 1901414 (2020). https://doi.org/10.1002/adfm.201901414

Das, S., Bandyopadhyay, A., Das, S., Das, D., Sutradhar, S.: Defect induced room-temperature ferromagnetism and enhanced dielectric property in nanocrystalline ZnO co-doped with Tb and Co. J. Alloys Comp. **731**, 591 (2018). https://doi.org/10.1016/j.jallcom.2017.10.057

De AlmeidaV, M., Mesquita, A., de Zevallos, A.O., Mamani, N.C., Neves, P.P., Gratens, X., et al.: Room temperature ferromagnetism promoted by defects at zinc sites in Mn-doped ZnO. J. Alloys Comp. **655**, 406 (2016). https://doi.org/10.1016/j.jallcom.2015.09.084

Delgado, F.P., Vasquez, F.C., Momaca, J.T.H., Rodríguez, C.R.S., Aquino, J.A.M., Méndez, S.F.O.: Room-temperature ferromagnetism and morphology evolution of SnO_2 flower-like microparticles by Zn-doping. J. Magnet. Mag. Mater. **476**, 183 (2019). https://doi.org/10.1016/j.jmmm.2018.12.102

Deng, S.Z., Fan, H.M., Wang, M., Zheng, M.R., Yi, J.B., Wu, R.Q.: Thiol-capped ZnO nanowire/nanotube arrays with tunable magnetic properties at room temperature. ACS Nano **4**, 495 (2010). https://doi.org/10.1021/nn901353x

Deng, N., Li, J., Hong, B., Jin, D., Peng, X., Wang, X., et al.: Nanocasting synthesis of co-doped In_2O_3: a 3D diluted magnetic semiconductor composed of nanospheres. J. Nanopart. Res. **17**, 191 (2015). https://doi.org/10.1007/s11051-015-2987-4

Dey, B., Narzary, R., Panda, S.K., Mallick, J., Mondal, A., Ravi, S., et al.: Room temperature d^0 ferromagnetism, band-gap reduction, and high optical transparency in p-type K-doped ZnO compounds for spintronics applications. Mater. Sci. Semicond. Process. **148**, 106798 (2022). https://doi.org/10.1016/j.mssp.2022.106798

Dhamodaran, M., Karuppannan, R., Murugan, R., Boukhvalov, D.W., Pandian, M.S., Perumalsamy, R.: Morphology controlled synthesis of Fe and Mn co-doped In_2O_3 nanocubes and their Dopant-Atom effects on electronic structure and magnetic properties. J. Magnet. Magnetic Mater. **560**, 169547 (2022). https://doi.org/10.1016/j.jmmm.2022.169547

Dhiman, P., Batoo, K.M., Kotnala, R.K., Chand, J., Singh, M.: Room temperature ferromagnetism and structural characterization of Fe, Ni co-doped ZnO nanocrystals. Appl. Surf. Sci. **287**, 287 (2013). https://doi.org/10.1016/j.apsusc.2013.09.144

Dietl, T., Ohno, H., Matsukura, F., Cibert, J., Ferrand, D.: Zener model description of ferromagnetism in zinc-blende magnetic semiconductors. Science **287**, 1019–1022 (2000). https://doi.org/10.1126/science.287.5455.1019

Dolai, S., Sarangi, S.N., Hussain, S., Bhar, R., Pal, A.K.: Magnetic properties of nanocrystalline nickel incorporated CuO thin films. J. Magn. Magn. Mater. **479**, 59 (2019). https://doi.org/10.1016/j.jmmm.2019.02.005

Dorneanu, P.P., Airinei, A., Grigoras, M., Fifere, N., Sacarescu, L., Lupu, N., et al.: Structural, optical and magnetic properties of Ni doped SnO_2 nanoparticles. J. Alloys Comp. **688**, 65 (2016). https://doi.org/10.1016/j.jallcom.2016.01.183

Du, C.L., Gu, Z.B., You, Y.M., Kasim, J., Yu, T., Shen, Z.X., et al.: Resonant Raman spectroscopy of (Mn, Co)-codoped ZnO films. J. Appl. Phys. **103**, 023521 (2008). https://doi.org/10.1063/1.2837110

Duhalde, S., Vignolo, M.F., Golmar, F., Chiliotte, C., Torres, C.E.R., Errico, L.A.: Appearance of room-temperature ferromagnetism in Cu-doped $TiO_{2-\delta}$ films. Phys. Rev. B **72**, 161313(R) (2005). https://doi.org/10.1103/physrevb.72.161313

Fazariah, N., Prabowo, W.A.E., Fathurrahman, F., Melati, A., Dipojono, H.K.: The investigation of electronic structure of transition metal doped TiO_2 for diluted magnetic semiconductor applications: a first principle study. Proced. Eng. **170**, 141 (2017). https://doi.org/10.1016/j.proeng.2017.03.032

Fitzgerald, C.B., Venkatesan, M., Dorneles, L.S., Gunning, R., Stamenov, P., Coey, J.M.D.: Magnetism in dilute magnetic oxide thin films based on SnO_2. Phys. Rev. B **74**, 115307 (2006). https://doi.org/10.1103/PhysRevB.74.115307

Fukumura, T., Yamada, Y., Toyosakin, H., Hasegawa, T., Koinuma, H., Kawasaki, M.: Exploration of oxide-based diluted magnetic semiconductors toward transparent spintronics. Appl. Surf. Sci. **223**, 62 (2004). https://doi.org/10.1016/S0169-4332(03)00898-5

Fukumura, T., Toyosaki, H., Ueno, K., Nakano, M., Kawasaki, M.: Role of charge carriers for ferromagnetism in cobalt-doped rutile TiO2. New J. Phys. **10**, 055018 (2008). https://doi.org/10.1088/1367-2630/10/5/055018

Gao, D., Zhang, J., Yang, G., Zhang, J., Shi, Z., Qi, J., et al.: Ferromagnetism in ZnO nanoparticles induced by doping of a nonmagnetic element: Al. J. Phys. Chem. C **114**, 13477 (2010a). https://doi.org/10.1021/jp103458s

Gao, D., Yang, G., Li, J., Zhang, J., Zhang, J., Xue, D.: Room-temperature ferromagnetism of flowerlike CuO nanostructures. J. Phys. Chem. C **114**, 18347–18351 (2010b). https://doi.org/10.1021/jp106015t

Ghosh, B., Sardar, M., Banerjee, S.: Destruction of ferromagnetism in Cu-doped ZnO upon thermal annealing: role of oxygen vacancy. J. Phys. D Appl. Phys. **46**, 135001 (2013). https://doi.org/10.1088/0022-3727/46/13/135001

Gu, H., Jiang, Y., Yan, M.: Defect-induced room temperature ferromagnetism in Fe and Na co-doped ZnO nanoparticles. J. Alloys Comp. **521**, 90 (2012a). https://doi.org/10.1016/j.jallcom.2012.01.043

Gu, H., Jiang, Y., Xu, Y., Yan, M.: Effect of defects on room-temperature ferromagnetism in Co and Na co-doped ZnO. Appl. Phys. A **107**, 919 (2012b). https://doi.org/10.1007/s00339-012-6824-7

Guillen, J.O., Lany, S., Barabash, S.V., Zunger, A.: Magnetism without magnetic ions: percolation, exchange, and formation energies of magnetism-promoting intrinsic defects in CaO. Phys. Rev. Lett. **96**, 107203 (2006). https://doi.org/10.1103/physrevlett.96.107203

Gupta, R., Brown, D., Ghosh, K., Mishra, S.R., Kahol, P.K.: Magneto-transport properties of Gd-doped In_2O_3 thin films. MRS Online Proc. Libr. **1032**, 604 (2007). https://doi.org/10.1557/PROC-1032-I06-04

Gupta, A., Zhang, R., Kumar, P., Kumar, V., Kumar, A.: Nano-structured dilute magnetic semiconductors for efficient spintronics at room temperature. Magnetochemistry **6**, 15 (2020). https://doi.org/10.3390/magnetochemistry6010015

Guuillen, J.O., Lany, S., Zunger, A.: Atomic control of conductivity versus ferromagnetism in wide-gap oxides via selective doping: V, Nb, Ta in Anatase TiO_2. Phys. Rev. Lett. **100**, 036601 (2008). https://doi.org/10.1103/physrevlett.100.036601

Han, D.S., Park, J.: Ferromagnetic Mn-doped GaN nanowires. Appl. Phys. Lett. **86**, 032506 (2005). https://doi.org/10.1063/1.1852725

He, J., Xu, S., Yoo, Y.K., Xue, Q., Lee, H.C., Cheng, S., et al.: Room temperature ferromagnetic *n*n-type semiconductor in $(In_{1-x}Fe_x)_2O_{3-\sigma}$. Appl. Phys. Lett. **86**, 052503 (2005). https://doi.org/10.1063/1.1851618

Heo, Y.W., Norton, D.P., Tien, L.C., Kwon, Y., Kang, B.S., Ren, F., et al.: ZnO nanowire growth and devices. Mater. Sci. Eng. R 47, 1 (2004). https://doi.org/10.1016/j.mser.2004.09.001

Herng, T.S., Lau, S.P., Yu, S.F., Tsang, S.H., Teng, K.S., Chen, J.S.: Ferromagnetic Cu doped ZnO as an electron injector in heterojunction light emitting diodes. J. Appl. Phys. **104**, 103104 (2008). https://doi.org/10.1063/1.3021142

Hoa, N.T.Q., Hiyen, D.N.: Comparative study of room temperature ferromagnetism in undoped and Ni-doped TiO_2 nanowires synthesized by solvothermal method. J. Mater. Sci. Mater. Electron. **24**, 793 (2013). https://doi.org/10.1007/s10854-012-0811-9

Holub, M., Bhattacharya, P.: Spin-polarized light-emitting diodes and lasers. J. Phys. D Appl. Phys. **40**, R179 (2007). https://doi.org/10.1088/0022-3727/40/11/R01

Hong, N.H., Sakai, J., Prellier, W.: Distribution of dopant in Fe:TiO_2 and Ni:TiO_2 thin films. J. Magnet. Magn. Mater. **281**, 347–352 (2004). https://doi.org/10.1016/j.jmmm.2004.04.125

Hong, N.H., Sakai, J., Brize, V.: Observation of ferromagnetism at room temperature in ZnO thin films. J. Phy. Condens. Matter. **19**, 036219 (2007). https://doi.org/10.1088/0953-8984/19/3/036219

Hou, D., Meng, H.J., Jia, L.Y., Ye, X.J., Zhou, H.J., Li, X.L.: Oxygen vacancy enhanced the room temperature ferromagnetism in Ni-doped TiO_2 thin films. Phys. Lett. A **364**, 318 (2007a). https://doi.org/10.1016/j.physleta.2006.11.077

Hou, D.L., Meng, H.J., Jia, L.Y., Ye, X.J., Zhou, H.J., Li, X.L.: Impurity concentration study on ferromagnetism in Cu-doped TiO_2 thin films. Europhys. Lett. **78**, 67001 (2007b). https://doi.org/10.1209/0295-5075/78/67001

Houssa, M., Iordanidou, K., Pourtois, G., Afanas'ev, V.V., Stesmans, A.: Ferromagnetism in two-dimensional hole-doped SnO. AIP Adv. **8**, 055010 (2018). https://doi.org/10.1063/1.5025272

In-Bo, S., Kim, C.S.: Doping effect of indium oxide-based diluted magnetic semiconductor thin films. J. Magn. Magn. Mater **272–276**, E1571–E1572 (2004). https://doi.org/10.1016/j.jmmm.2003.12.1370

Iqbal, M., Fatheema, J., Noor, Q., Rani, M., Mumtaz, M., Zheng, R.K., et al.: Co-existence of magnetic phases in two-dimensional MXene. Mater. Today Chem. **16**, 100271 (2020). https://doi.org/10.1016/j.mtchem.2020.100271

Jadhav, J., Biswas, S.: Shape-controlled magnetic nanoplatelets of Ni-doped ZnO synthesized via a chemical precursor. J. Alloys Comp. **664**, 71 (2016). https://doi.org/10.1016/j.jallcom.2015.12.191

Jayabharathi, J., Karunakaran, C., Kalaiarasi, V., Ramanathan, P.: Nano ZnO, Cu-doped ZnO, and Ag-doped ZnO assisted generation of light from imidazole. J. Photochem. Photobiol. A Chem. **295**, 1–10 (2014). https://doi.org/10.1016/j.jphotochem.2014.09.002

Jayakumar, O.D., GopalakrishanI, K., Kadam, R.M., Vinu, A., Asthana, A., Tyagi, A.K.: Magnetization and structural studies of Mn Doped ZnO nanoparticles: prepared by reverse micelle method. J. Cryst. Growth **300**, 358–363 (2007). https://doi.org/10.1016/j.jcrysgro.2006.12.030

Jing, D., Zhang, Y., Guo, L.: Study on the synthesis of Ni doped mesoporous TiO_2 and its photocatalytic activity for hydrogen evolution in aqueous methanol solution. Chem. Phys. Lett. **415**, 74 (2005). https://doi.org/10.1016/j.cplett.2005.08.080

Kamble, S.P., Mote, V.D.: Optical and room-temperature ferromagnetic properties of Ni-doped CuO nanocrystals prepared via auto-combustion method. J. Mater. Sci. Mater. Electron. **32**, 5309 (2021). https://doi.org/10.1007/s10854-020-05106-8

Kanwal, S., Khan, M.T., Mehboob, N., Amami, M., Zaman, A.: Room-temperature ferromagnetism in Cu/Co Co-doped ZnO nanoparticles prepared by the co-precipitation method: for spintronics applications. ACS Omega **7**, 32184 (2022). https://doi.org/10.1021/acsomega.2c03375

Kayani, Z.N., Anwar, M., Saddiqe, Z., Riaz, S., Naseem, S.: Biological and optical properties of sol–gel derived ZnO using different percentages of silver contents. Colloids Surf. B **171**, 383 (2018). https://doi.org/10.1016/j.colsurfb.2018.07.055

Kayani, Z.N., Usman, A., Nazli, H., Riffat, S., Riaz, S., Naseem, S.: Dielectric and magnetic properties of dilute magnetic semiconductors Ag-doped ZnO thin films. Appl. Phys. A **126**, 559 (2020). https://doi.org/10.1007/s00339-020-03748-3

Khan, R., Hu, F.M.: Dielectric and magnetic properties of (Zn, Co) co-doped SnO_2 nanoparticles. Chin. Phys. B **24**, 127803 (2015). https://doi.org/10.1088/1674-1056/24/12/127803

Khan, Z.H., Islamuddin, K.R.K., Salah, N., Habib, S., Hamidy, S.M.A., et al.: Optical and electrical characterization of ZnO thin film. Int. J. Nanosci. **9**, 423 (2010). https://doi.org/10.1142/S0219581X10007083

Khan, R., Fashu, S., Zaman, Y.: Magnetic and dielectric properties of (Co, Zn) co-doped SnO2 diluted magnetic semiconducting nanoparticles. J. Mater. Sci. Mater. Electron. **27**, 5960–5966 (2016a). https://doi.org/10.1007/s10854-016-4517-2

Khan, R., Rahman, M.U., Rahman, Z.U., Fashu, S.: Effect of air annealing on the structure, dielectric and magnetic properties of (Co, Ni) co-doped SnO2 nanoparticles. J. Mater. Sci. Mater. Electron. **27**, 10532–10540 (2016b). https://doi.org/10.1007/s10854-016-5144-7

Kim, K.J., Park, Y.R.: Spectroscopic ellipsometry study of optical transitions in $Zn_{1-x}CO_xO$ alloys. Appl. Phys. Lett. **81**, 1420 (2002). https://doi.org/10.1063/1.1501765

Kim, S.W., Lee, S., Saqib, A.N.S., Lee, Y.H.: Ferromagnetism in undoped ZnO nanostructures synthesized by solution plasma process. Current Appl. Phys. **17**, 181 (2016). https://doi.org/10.1016/j.cap.2016.11.016

Köseoğlu, Y.: Rapid synthesis of room temperature ferromagnetic Fe and Co co-doped ZnO DMS nanoparticles. Ceram. Int. **41**, 11655 (2015). https://doi.org/10.1016/j.ceramint.2015.05.127

Kumar, S., Basu, S., Rana, B., Barman, A., Chatterjee, S., Jha, S.N., et al.: Structural, optical and magnetic properties of sol-gel derived ZnO: co diluted magnetic semiconductor nanocrystals: an EXAFS study. J. Mater. Chem. C **2**, 481 (2014). https://doi.org/10.1039/C3TC31834F

Kumar, S., Tiwari, N., Jha, S.N., Chatterjee, S., Bhattacharya, D., Ghosh, A.K.: Structural and optical properties of sol-gel derived cr-doped ZnO diluted magnetic semiconductor nanocrystals: an EXAFS study to relate the local structure. RSC Adv. **6**, 107816 (2016). https://doi.org/10.1039/C6RA15685A

Kumar, A., Kashyap, M.K., Sabharwal, N., Kumar, S., Kumar, A., Kumar, P., et al.: Structural, optical and weak magnetic properties of Co and Mn codoped TiO2 nanoparticles. Solid State Sci. **73**, 19 (2017). https://doi.org/10.1016/j.solidstatesciences.2017.09.002

Kumar, A., Kumar, M., Sati, P.C., Srivastava, M.K., Ghosh, S., Kumar, S.: Structural, magnetic and optical properties of diluted magnetic semiconductor (DMS) phase of Ni modified CuO nanoparticles. Curr. Appl. Phys. **32**, 24 (2021). https://doi.org/10.1016/j.cap.2021.09.002

Kumar, V., Singh, S., Kumar, P.: Room temperature ferromagnetism in chemically synthesized ZnO nanoparticles. J. Ultra Sci. Phys. Sci. **34**, 42 (2022). https://doi.org/10.22147/jusps-A/340301

Kumbhakar, P., Gowda, C.C., Mahapatra, P.L., Mukherjee, M., Malviya, K.D., Chaker, M.: Emerging 2D metal oxides and their applications. Mater. Today **45**, 142 (2021). https://doi.org/10.1016/j.mattod.2020.11.023

Kvashnin, D.G., Kvashnin, A.G., Kano, E., Hashimoto, A., Takeguchi, M., Naramoto, H.: Two-dimensional CuO inside the supportive bilayer graphene matrix. J. Phys. Chem. C **123**, 17459 (2019). https://doi.org/10.1021/acs.jpcc.9b05353.s001

Lekshmy, S.N.S., Anitha, V.S.N., Vargehese, T.P.K., Joy, K.: Magnetic properties of Mn-Doped SnO_2 thin films prepared by the sol-gel dip coating method for dilute magnetic semiconductors. J. Am. Ceram. Soc. **97**, 3184 (2014). https://doi.org/10.1111/jace.13084

Levard, C., Reinsch, B.C., Michel, F.M., Oumahi, C., Lowry, G.V., Brown, G.E., Jr.: Sulfidation processes of PVP-coated silver nanoparticles in aqueous solution: impact on dissolution rate. Environ. Sci. Technol. **45**, 5260–5266 (2011). https://doi.org/10.1021/es2007758

Li, X., Xia, C., Pei, G., He, X.: Synthesis and characterization of room-temperature ferromagnetism in Fe- and Ni-co-doped In2O3. J. Phys. Chem. Solids **68**, 1836–1840 (2007). https://doi.org/10.1016/j.jpcs.2007.05.019

Li, H., Song, B., Bao, H.Q., Wang, G., Wang, W.J., Chen, X.L.: Ferromagnetism of Mn-doped GaN polycrystalline powders. J. Magn. Magn. Mater. **321**, 222–225 (2009). https://doi.org/10.1016/j.jmmm.2008.09.016

Li, Y., Xu, M., Pan, L., Zhang, Y., Guo, Z., Bi, C.: Structural and room-temperature ferromagnetic properties of Fe-doped CuO nanocrystals. J. Appl. Phys. **107**, 113908 (2010). https://doi.org/10.1063/1.3436573

Li, W.J., Kong, C.Y., Ruan, H.B., Qin, G.P., Huang, G.J., Yang, T.Y., et al.: Electrical properties and raman scattering investigation of Ag doped ZnO thin films. Solid State Commun. **152**, 147 (2012). https://doi.org/10.1016/j.ssc.2011.10.006

Li, Y., Li, J., Yu, Z., Li, W., Zhu, M., Jin, H., et al.: Study on the high magnetic field processed ZnO based diluted magnetic semiconductors. Ceram. Int. **45**, 19583 (2019). https://doi.org/10.1016/j.ceramint.2019.07.011

Lin, X., Yang, W., Wang, K.L., Zhao, W.: Two-dimensional spintronics for low-power electronics. Nat. Electron. **2**, 274 (2019). https://doi.org/10.1038/s41928-019-0273-7

Liu, S.M., Gu, S.L., Ye, J.D., Zhu, S.M., Liu, W., Tang, K., et al.: Room-temperature ferromagnetism in Mn-N Co-doped p-ZnO epilayers by metal-organic chemical vapor deposition. Appl. Phys. A **91**, 535 (2008). https://doi.org/10.1007/s00339-008-4444-z

Liu, W., Zhang, H., Shi, J., Wang, Z., Song, C., Wang, X., et al.: A room-temperature magnetic semiconductor from a ferromagnetic metallic glass. Nat. Commun. **7**, 13497 (2016). https://doi.org/10.1038/ncomms13497

Liu, X., Zhang, S., Wu, Z., An, Y.: Manganese-vacancy complexes induced room temperature ferromagnetism in Mn/Mg co-doped In_2O_3 diluted magnetic semiconductors. Superlattices Microstruct. **132**, 106174 (2019). https://doi.org/10.1016/j.spmi.2019.106174

M'aca, F., Kudrnovský, J., Drchal, V., Bouzerar, G.: Magnetism without magnetic impurities in ZrO2 oxide. Appl. Phys. Lett. **92**, 212503 (2008). https://doi.org/10.1063/1.2936858

Ma, X., Lou, C.: The dilute magnetic and optical properties of Mn-doped ZnO nanowires. J. Nanomater. **2011**, 464538 (2011). https://doi.org/10.1155/2011/464538

Maca, F., Kudrnovsky, J., Drchal, V., Bouzerar, G.: Magnetism without magnetic impurities in oxides ZrO_2 and TiO_2. Philos. Mag. A **88**, 2755 (2008). https://doi.org/10.1080/14786430802342584

Mahmoud, W.E.: Synthesis and optical properties of Ce-doped ZnO hexagonal nanoplatelets. J. Cryst. Growth **312**, 3075–3079 (2010). https://doi.org/10.1016/j.jcrysgro.2010.07.040

Mahmoud, W.E., Al-Marzouski, F., Al-Ameer, S., Al-Hazmi, F.: Synthesis and characterization of one-dimensional vertically aligned Sb-doped ZnO nanowires. J. Appl. Crystallogr. **5**, 182 (2012). https://doi.org/10.1107/S0021889812001665

Manikandan, D., Murugan, R.: Room temperature dilute magnetism in nanoscale Co and Zn co-doped SnO2. Superlattices Microstruct. **89**, 7 (2016). https://doi.org/10.1016/j.spmi.2015.10.045

Manna, S., De, S.K.: Room temperature ferromagnetism in Fe doped CuO nanorods. J. Magnet. Magn. Mater. **322**, 2749–2753 (2010). https://doi.org/10.1016/j.jmmm.2010.04.020

Manzoor, M., Rafiq, A., Ikram, M., Nafees, M., Ali, S.: Structural, optical, and magnetic study of Ni-doped TiO_2 nanoparticles synthesized by sol–gel method. Int. Nano Lett. **8**, 1–8 (2018). https://doi.org/10.1007/s40089-018-0225-7

Matsumoto, Y., Murakami, M., Shono, T., Hasegawa, T., Fukumra, T., Kawasaki, M., et al.: Room-temperature ferromagnetism in transparent transition metal-doped titanium dioxide. Science **291**, 854 (2001). https://doi.org/10.1126/science.1056186

Medhi, R., Marquez, M.D., Lee, T.R.: Visible-light-active doped metal oxide nanoparticles: review of their synthesis, properties, and applications. ACS Appl. Nano Mater. **3**, 6156 (2020). https://doi.org/10.1021/acsanm.0c01035

Mehraj, S., Ansari, M.S.: Structural, electrical and magnetic properties of (Fe, Co) co-doped SnO2 diluted magnetic semiconductor nanostructures. Phys. E **65**, 84 (2015). https://doi.org/10.1016/j.physe.2014.08.016

Meneses, C.T., Duque, J.G.S., Vivas, L.G., Knobel, M.: Synthesis and characterization of TM-doped CuO (TM = Fe, Ni). J. Noncryst. Solids **354**, 4830–4832 (2008). https://doi.org/10.1016/j.jnoncrysol.2008.04.025

Morozov, I.G., Belousova, O.V., Sathasivam, S., Parkin, I.P., Kuznetsov, M.V.: Some peculiarities of room-temperature ferromagnetism in ensembles of mixed-phase TiN_x-TiO_y nanoparticles. Mater. Res. Bull. **134**, 111092 (2021). https://doi.org/10.1016/j.materresbull.2020.111092

Motaung, D.E., Mhlongo, G.H., Nkosi, S.S., Malgas, G.F., Mwakikunga, B.W., Coetsee, E., et al.: Shape-selective dependence of room temperature ferromagnetism induced by hierarchical ZnO nanostructures. ACS Appl. Mater. Interfaces **6**, 8981 (2014). https://doi.org/10.1021/am501911y

Mudarra Navarro, A.M., Rodríguez Torres, C.E., Bilovol, V., Fabiana Cabrera, A., Errico, L., Weissmann, M.: Study of the relation between oxygen vacancies and ferromagnetism in undoped and Fe-doped TiO_2 nanoparticles. J. Appl. Phys. **115**, 223908 (2014). https://doi.org/10.1063/1.4883183

Nachiar, R.A., Muthukumaran, S.: Structural, photoluminescence and magnetic properties of Cu-doped SnO2 nanoparticles co-doped with Co. Opt. Laser Tech. **112**, 458–466 (2019). https://doi.org/10.1016/j.optlastec.2018.11.055

Nagal, V., Khan, M.S., Kumar, V., Boora, N., Khan, Z.H., Singh, K., et al.: Optical study of ZnO nanorods grown by vapour solid growth method for energy harvesting applications. AIP Conf. Proc. **2276**, 020022 (2020). https://doi.org/10.1063/5.0025737

Narzary, R., Dey, B., Chouhan, L., Kumar, S., Ravi, S., Srivastava, S.K.: Optical band gap tuning, zero dielectric loss and room temperature ferromagnetism in (Ag/Mg) co-doped SnO_2 compounds for spintronics applications. Mater. Sci. Semicond. Process. **142**, 106477 (2022). https://doi.org/10.1016/j.mssp.2022.106477

Naseem, S., Khan, W., Khan, S., Husain, S., Ahmad, A.: Consequences of (Cr/Co) co-doping on the microstructure, optical and magnetic properties of microwave assisted sol-gel derived TiO_2 nanoparticles. J. Lumines. **205**, 406 (2019). https://doi.org/10.1016/j.jlumin.2018.09.022

Ning, S., Zhan, P., Xie, Q., Li, Z., Zhang, Z.: Room-temperature ferromagnetism in un-doped ZrO_2 thin films. J. Phys. D Appl. Phys. **46**, 445004 (2013). https://doi.org/10.1088/0022-3727/46/44/445004

Nomura, K., Okabayashi, J., Okamura, K., Yamada, Y.: Magnetic properties of Fe and Co codoped SnO2 prepared by sol-gel method. J. Appl. Phys. **110**, 083901 (2011). https://doi.org/10.1063/1.3651468

Nunes, M.R., Monteiro, O.C., Castro, A.L., Vasconcelos, D.A., Silvestre, A.J.: A new chemical route to synthesise TM-doped (TM = Co, Fe) TiO_2 nanoparticles. Eur. J. Inorg. Chem. **2008**, 961 (2008). https://doi.org/10.1002/ejic.200700978

Okabayashi, J., Nomura, K., Kono, S., Yamada, Y.: Magnetization enhancement in room-temperature ferromagnetic Fe–Mn Co-Doped SnO_2. Japan J. Appl. Phys. **51**, 023003 (2012). https://doi.org/10.1143/JJAP.51.023003

Oliveira, A.A., Valerio-Cuadros, M.I., Tupan, L.F.S., Zanuto, V.S., Ivashita, F.F., Paesano, A., Jr.: Fe-doped In_2O_3 nanostructures synthesized via a freeze-drying process: structural and optical properties. Mater. Lett. **250**, 210 (2019). https://doi.org/10.1016/j.matlet.2019.05.025

Oliveira, A.A., Valerio-Cuadros, M.I., de Brito, A.S., Tupan, L.F.S., Barco, R., Ivashita, F.F., et al.: Magnetic behavior and site occupancy in Fe-doped In_2O_3 nanoparticles. J. Magn. Magn. Mater **547**, 168944 (2022). https://doi.org/10.1016/j.jmmm.2021.168944

Pan, F., Song, C., Liu, X.J., Yang, Y.C., Zeng, F.: Ferromagnetism and possible application in spintronics of transition-metal-doped ZnO films. Mater. Sci. Eng. R Rep. **62**, 1 (2008). https://doi.org/10.1016/j.mser.2008.04.002

Parveen, B., Hassan, M., Khalid, Z., Riaz, S., Naseem, S.: Room-temperature ferromagnetism in Ni-doped TiO_2 diluted magnetic semiconductor thin films. J. Appl. Res. Tech. **15**, 132 (2017). https://doi.org/10.1016/j.jart.2017.01.009

Pearton, S.J., Norton, D.P., Ivill, M.P., Hebard, A.F., Chen, M.W., Buyanova, A.I., et al.: Transition metal doped ZnO for spintronics. MRS Online Proc. Libr. **999**, 304 (2007). https://doi.org/10.1557/PROC-0999-K03-04

Peleckis, G., Wang, X.L., Dou, S.X.: Room-temperature ferromagnetism in Mn and Fe codoped In_2O_3. Appl. Phys. Lett. **88**, 132507 (2006). https://doi.org/10.1063/1.2191093

Pemmaraju, C.D., Sanvito, S.: Ferromagnetism driven by intrinsic point defects in HfO_2. Phys. Rev. Lett. **94**, 217205 (2005). https://doi.org/10.1103/physrevlett.94.217205

Peng, H., Li, J., Li, S.S., Xia, J.B.: Possible origin of ferromagnetism in undoped anatase TiO_2. Phys. Rev. B **79**, 092411 (2009). https://doi.org/10.1103/physrevb.79.092411

Phan, T.L., Nghia, N.X., Yu, S.C.: Raman scattering spectra and magnetic properties of polycrystalline $Zn_{1-x}Co_xO$ ceramics. Solid State Commun. **152**, 2087–2091 (2012). https://doi.org/10.1016/j.ssc.2012.08.026

Phan, T.L., Zhang, Y.D., Yang, D.S., Nghia, N.X., Thanh, T.D., Yu, S.C.: Defect-induced ferromagnetism in ZnO nanoparticles prepared by mechanical milling. Appl. Phys. Lett. **102**, 072408 (2013). https://doi.org/10.1063/1.4793428

Prajapati, B., Kumar, S., Kumar, M., Chatterjee, S., Ghosh, A.K.: Investigation of the physical properties of Fe:TiO_2–diluted magnetic semiconductor nanoparticles. J. Mater. Chem. C **5**, 4257 (2017). https://doi.org/10.1039/C7TC00233E

Prakash, R., Kumar, S., Ahmad, F., Lee, C.G., Song, J.I.: Room temperature ferromagnetism in Ni doped In2O3 nanoparticles. Thin Solid Films **519**, 8243 (2011). https://doi.org/10.1016/j.tsf.2011.03.105

Prestgard, M.C., Siegel, G.P., Tiwari, A.: Oxides for spintronics: a review of engineered materials for spin injection. Adv. Mat. Lett. **5**, 242 (2014). https://doi.org/10.5185/AMLETT.2014.AMWC1032

Rahman, M., Saqib, M., Althubeiti, K., Abualnaja, K.M., Zaman, S., Rahman, N., et al.: Effect of Sr and Co co-doping on the TiO_2-diluted magnetic semiconductor for spintronic applications. J. Mater. Sci. Mater. Electron. **32**, 28718 (2021). https://doi.org/10.1007/s10854-021-07253-y

Rai, D.P., Laref, A., Shanker, A., Sandeep, S.A., Khenata, R., Thapa, R.K.: Spin-induced transition metal (TM) doped SnO_2 a dilute magnetic semiconductor (DMS): A first principles study. Phys. Chem. Solids **120**, 104–108 (2018). https://doi.org/10.1016/j.jpcs.2018.04.006

Rana, A.K., Kumar, Y., Rajput, P., Jha, S.N., Bhattacharyya, D., Shirage, P.M.: Search for origin of room temperature ferromagnetism properties in Ni-doped ZnO nanostructure. ACS Appl. Mater. Interfaces **9**, 7691 (2017). https://doi.org/10.1021/acsami.6b12616

Ravi, S., Shashikanth, F.W.: Ferromagnetism in Mn doped Copper Oxide nanoflake like structures with high Neel temperature. Mater. Lett. **141**, 132 (2015). https://doi.org/10.1016/j.matlet.2014.11.089

Ren, H., Xiang, G.: Morphology-dependent room-temperature ferromagnetism in undoped ZnO nanostructures. Nanomaterials **11**, 3199 (2021). https://doi.org/10.3390/nano11123199

Rodriguez-Torres, C., Cabrera, A.F., Errico, L.A., Adán, C., Requejo, F.G., Weissmann, M., et al.: Local structure and magnetic behaviour of Fe-doped TiO_2 anatase nanoparticles: experiments and calculations. J. Phys. Condens. Matter. **20**, 135210 (2008). https://doi.org/10.1088/0953-8984/20/13/135210

Sakai, E., Chikamatsu, A., Hirose, Y., Shimada, T., Hasegawa, T.: Magnetic and transport properties of anatase TiO_2 codoped with Fe and Nb. Appl. Phys. Express **3**, 043001 (2010). https://doi.org/10.1143/APEX.3.043001

Salah, N., Habib, S.S., Khan, Z.H., Memic, A., Azam, A., Alarfaj, E., et al.: High-energy ball milling technique for ZnO nanoparticles as antibacterial material. Int. J. Nanomed. **6**, 863 (2011). https://doi.org/10.2147/IJN.S18267

Salah, N., Habib, S., Azam, A.: The influence of transition metal doping on the thermoelectric and magnetic properties of microwave synthesized SnO_2 nanoparticles. J. Mater. Sci. Mater. Electron. **28**, 435 (2017). https://doi.org/10.1007/s10854-016-5540-z

Santara, B., Giri, P.K., Dhara, S., Imakita, K., Fujii, M.: Oxygen vacancy-mediated enhanced ferromagnetism in undoped and Fe-doped TiO_2 nanoribbons. J. Phys. D Appl. Phys. **47**, 235304 (2014). https://doi.org/10.1088/0022-3727/47/23/235304

Satheesan, M.K., Vani, K., Kumar, V.: Acceptor-defect mediated room temperature ferromagnetism in (Mn2+, Nb5+) co-doped ZnO nanoparticles. Ceram. Int. **43**, 8098 (2017). https://doi.org/10.1016/j.ceramint.2017.03.132

Schmidt, G., Molenkamp, L.W.: Dilute magnetic semiconductors in spin-polarized electronics. J. Appl. Phys. **89**, 7443 (2001). https://doi.org/10.1063/1.1361053

Schmidt, T.M., Miwa, R.H., Fazzio, A.: Ferromagnetic coupling in a Co-doped graphene like ZnO sheet. Phys. Rev. B **81**, 195413 (2010). https://doi.org/10.1103/PhysRevB.81.195413

Schmidt-Mende, L., MacManus-Driscoll, J.L.: ZnO-nanostructures, defects and devices. Mater. Today **10**, 40 (2007). https://doi.org/10.1016/S1369-7021(07)70078-0

Sharma, P., Gupta, A., Rao, K.V., Owens, F.J., Sharma, R., Ahuja, R., et al.: Ferromagnetism above room temperature in bulk and transparent thin films of Mn-doped ZnO. Nat. Mater. **2**, 673–677 (2003). https://doi.org/10.1038/nmat984

Sharma, P., GuptaA, O.F.J., Inoue, A., Rao, K.V.: Room temperature spintronic material- Mn-doped ZnO revisited. J. Magn. Magn. Mater. **282**, 115–121 (2004). https://doi.org/10.1016/j.jmmm.2004.04.028

Sharma, S., Chaudhary, S., Kashyap, S.C., Sharma, S.K.: Room temperature ferromagnetism in Mn doped TiO_2 thin films: electronic structure and Raman investigations. J. Appl. Phys. **109**, 083905 (2011). https://doi.org/10.1063/1.3567938

Sharma, A., Tulapurkar, A.A., Muralidharan, B.: Resonant spin-transfer-torque nano-oscillators. Phys. Rev. Appl. **8**, 064014 (2017). https://doi.org/10.1103/PhysRevApplied.8.064014

Sheng, X., Chen, L., Xu, T., Zhu, K., Feng, X.: Understanding and removing surface states limiting charge transport in TiO_2 nanowire arrays for enhanced optoelectronic device performance. Chem. Sci. **7**, 1910–1913 (2016). https://doi.org/10.1039/C5SC04076K

Shin, S.W., Kim, I.Y., Jeon, K.S., Heo, J.Y., Heo, G.S., Patil, P.S., et al.: Wide band gap characteristic of quaternary and flexible Mg and Ga co-doped ZnO transparent conductive thin films. J. Asian Ceram. Soc. **1**, 262–266 (2013). https://doi.org/10.1016/j.jascer.2013.06.003

Siddheswaran, R., Mangalaraja, R.V., Gómez, M.E., Avila, R.E., Jeyanthi, C.E.: Room temperature ferromagnetism in combustion synthesized nanocrystalline Co, Al Co-Doped ZnO. J. Alloys Comp. **581**, 146 (2013). https://doi.org/10.1016/j.jallcom.2013.06.117

Singh, J.P., Chae, K.H.: d^0 ferromagnetism of magnesium oxide. Condens. Matter **2**, 36 (2017). https://doi.org/10.3390/condmat2040036

Song, T., Cai, X., Tu, M.W.-Y., Zhang, X., Huang, B., Wilson, N.P., et al.: Giant tunneling magnetoresistance in spin-filter van der Waals heterostructures. Science **360**, 1214 (2018). https://doi.org/10.1126/science.aar4851

Srinet, G., Sharma, S., Sanchez, J.G., Diazd, R.G., Perez, R.P., Siqueiros, J.M., et al.: Room-temperature ferromagnetism on ZnO nanoparticles doped with Cr: an experimental and theoretical analysis. J. Alloys Comp. **849**, 156587 (2020). https://doi.org/10.1016/j.jallcom.2020.156587

Srivastava, S.K., Lejay, P., Barbara, B., Pailh'es, S., Madigou, V., Bouzerar, G.: Possible room-temperature ferromagnetism in K-doped SnO_2: X-ray diffraction and high-resolution transmission electron microscopy study. Phys. Rev. B **82**, 193203 (2010). https://doi.org/10.1103/physrevb.82.193203

Srivastava, S.K., Lejay, P., Barbara, B., Boisron, O., Pailh'es, S., Bouzerar, G.: Non-magnetic impurity induced magnetism in rutile TiO_2: K compounds. J. Phys. Condens. Matter **23**, 442202 (2011). https://doi.org/10.1088/0953-8984/23/44/442202

Srivastava, S.K., Lejay, P., Azzem, A.H., Bouzerar, G.: Non-magnetic impurity induced magnetism in Li-doped SnO_2 nanoparticles. J. Supercond. Nov. Magn. **27**, 487 (2013). https://doi.org/10.1007/s10948-013-2287-0

Sundaram, G.A., Yang, M., Nomura, K., Maniarasu, S., Veerappan, G., Liu, T., et al.: ^{119}Sn Mössbauer and ferromagnetic studies on hierarchical Tin- and nitrogen-codoped TiO_2 microspheres with efficient photocatalytic performance. J. Phys. Chem. C **121**, 6662 (2017). https://doi.org/10.1021/acs.jpcc.6b12397

Sundaresan, A., Bhargavi, R., Rangarajan, N., Siddesh, U., Rao, C.N.R.: Ferromagnetism as a universal feature of nanoparticles of the otherwise nonmagnetic oxides. Phys. Rev. B **74**, 161306 (2006a). https://doi.org/10.1103/PhysRevB.74.161306

Sundaresan, A., Bhargavi, R., Rangarajan, N., Siddesh, U., Rao, C.N.R.: Ferromagnetism as a universal feature of nanoparticles of the otherwise nonmagnetic oxides. Phys. Rev. B **74**, 161306 (2006b). https://doi.org/10.1103/PhysRevB.74.161306

Tan, H., Wang, C., Duan, H., Tian, J., Ji, Q., Lu, Y., et al.: Intrinsic room-temperature ferromagnetism in V_2C MXene nanosheets. ACS Appl. Mater. Interfaces **13**, 33363 (2021). https://doi.org/10.1021/acsami.1c07906

Tang, G., Shi, X., Huo, C., Wang, Z.: Room temperature ferromagnetism in hydrothermally grown Ni and Cu co-doped ZnO nanorods. Ceram. Int. **39**, 4825 (2013). https://doi.org/10.1016/j.ceramint.2012.11.073

Tao, J.G., Guan, L.X., Pan, J.S., Huan, C.H.A., Wang, L., Kuo, J.L.: Possible room temperature ferromagnetism of Li-doped anatase TiO_2: a first-principles study. Phys. Lett. **374**, 4451 (2010). https://doi.org/10.1016/j.physleta.2010.08.074

Tsai, S.P., Yang, C.Y., Lee, C.J., Lu, L.S., Liang, H.L., Lin, J.X., et al.: Room-temperature ferromagnetism of single-layer MoS_2 induced by antiferromagnetic proximity yttrium iron garnet. Adv. Quant. Tech. **4**, 2000104 (2021). https://doi.org/10.1002/qute.20200010

Venkatesan, M., Fitzgerald, C.B., Coey, J.M.D.: Unexpected magnetism in a dielectric oxide. Nature **430**, 630 (2004). https://doi.org/10.1038/430630a

Vijayaprasath, G., Murugan, R., Ravi, G., Mahalingam, T., Hayakawa, Y.: Characterization of dilute magnetic semiconducting transition metal doped ZnO thin films by sol-gel spin coating method. Appl. Surf. Sci. **313**, 870 (2014). https://doi.org/10.1016/j.apsusc.2014.06.093

Vizhi, R.E., Rajan, R.: Structural, optical and room temperature magnetic properties of sol–gel synthesized (Co, Fe) co-doped SnO_2 nanoparticles. J. Cryst. Growth **584**, 126565 (2022). https://doi.org/10.1016/j.jcrysgro.2022.126565

Wang, Y.S., Thomas, P.J., Brien, P.O.: Optical properties of ZnO nanocrystals doped with Cd, Mg, Mn, and Fe ions. J. Phys. Chem. B **110**, 21412 (2006). https://doi.org/10.1021/jp0654415

Wang, X.L., Zeng, Z., Zheng, X.H.: First-principles investigations of Co- and Fe-doped SnO_2. J. Appl. Phys. **101**, 09H104 (2007). https://doi.org/10.1063/1.2709740

Wang, X.L., Dai, Z.X., Zeng, Z.: Search for ferromagnetism in SnO2 doped with transition metals (V, Mn, Fe, and Co). J. Phys. Conden. Matter. **20**, 045214 (2008). https://doi.org/10.1088/0953-8984/20/04/045214

Wang, Y., Huang, Y., Song, Y., Zhang, X., Ma, Y., Liang, J., et al.: Room-temperature ferromagnetism of graphene. Nano Lett. **9**, 220 (2009). https://doi.org/10.1021/nl802810g

Wang, D., Chen, Z.Q., Wang, D.D., Qi, N., Gong, J., Cao, C.Y., et al.: Positron annihilation study of the interfacial defects in ZnO nanocrystals: correlation with ferromagnetism. J. Appl. Phys. **107**, 023524 (2010). https://doi.org/10.1063/1.3291134

Wang, K.L., Xiu, F., Jacob, A.P.: Spintronics of nanostructured manganese germanium (MnGe) dilute magnetic semiconductor. In: Shiraki, Y., Usami, N. (eds.) Woodhead Publishing Series in Electronic and Optical Materials, Silicon-Germanium (SiGe) Nanostructures, p. 575. Elsevier, Amsterdam (2011)

Wang, J., Hou, S., Chen, H., Xiang, L.: Defects-induced room temperature ferromagnetism in ZnO nanorods grown from ε-$Zn(OH)_2$. J. Phys. Chem. C **118**, 19469 (2014). https://doi.org/10.1021/jp5058226

Wang, C., Zhu, C., Lv, C., Li, D., Ma, X., Yang, D.: Electrically pumped random lasing from hydrothermal ZnO films of large grains. Appl. Surf. Sci. **332**, 620 (2015a). https://doi.org/10.1016/j.apsusc.2015.01.187

Wang, N., Zhou, W., Liang, Y., Cui, W., Wu, P.: Oxygen vacancy-mediated room temperature ferromagnetism in Sr-doped SnO_2 nanoparticles. J. Mater. Sci. Mater. Electron **26**, 7751–7756 (2015b). https://doi.org/10.1007/s10854-015-3420-6

Wang, Y., Nomura, K., Liu, X., Rykov, A.I., Jin, C., Liu, T., et al.: Structural and magnetic properties of ^{57}Fe-doped TiO_2 and ^{57}Fe/Sn-codoped TiO_2 prepared by a soft-chemical process. Eur. J. Inorg. Chem. **2016**, 2131 (2016). https://doi.org/10.1002/ejic.201501173

Wang, J., Zhou, D., Li, Y., Wu, P.: Experimental and first-principle studies of ferromagnetism in Na-doped SnO2 nanoparticles. Vacuum **141**, 62 (2017). https://doi.org/10.1016/j.vacuum.2017.03.024

Wang, Y.N., Jiang, F.X., Yan, L.J., Xu, X.H.: Magnetic and plasmonic properties in noncompensated Fe-Sn codoped In_2O_3 nanodot arrays. Appl. Surf. Sci. **441**, 415–419 (2018). https://doi.org/10.1016/j.apsusc.2018.02.050

Wang, J., Ma, L., Wang, X., Wang, X., Yao, J., Yi, Q., et al.: Sub-nanometer thick wafer-size NiO films with room-temperature ferromagnetic behaviour. Angew. Chem. Int. Ed. **60**, 25020 (2021). https://doi.org/10.1002/anie.202110185

Wangensteen, T., Dhakal, T., Merlak, M., Mukherjee, P., Phan, M., Chandra, S., et al.: Growth of uniform ZnO nanoparticles by a microwave plasma process. J. Alloys Compd. **509**, 6859 (2011). https://doi.org/10.1016/j.jallcom.2011.03.161

Wei, Y., Ke, L., Kong, J., Liu, H., Jiao, Z., Lu, X., et al.: Enhanced photoelectrochemical water-splitting effect with a bent ZnO nanorod photoanode decorated with Ag nanoparticles. Nanotechnology **23**, 235401 (2012). https://doi.org/10.1088/0957-4484/23/23/235401

Wu, C., Ding, W., Wang, F., Lu, Y., Yan, M.: Amorphousness induced significant room temperature ferromagnetism of TiO_2 thin films. Appl. Phys. Lett. **111**, 152408 (2017). https://doi.org/10.1063/1.4999912

Wu, H., Zhang, W., Yang, L., Wang, J., Li, J., Li, L., et al.: Strong intrinsic room-temperature ferromagnetism in free-standing non-van der Waals ultrathin 2D crystals. Nat. Commun. **12**, 5688 (2021). https://doi.org/10.1038/s41467-021-26009-0

Xi, L., Li-Ting, T., Wang, Y., Bao, N., Lu, Z., Ding, X., et al.: Intrinsic or interface clustering-induced ferromagnetism in Fe-doped In_2O_3- diluted magnetic semiconductors. ACS Appl. Mater. Interfaces **10**, 22372 (2018). https://doi.org/10.1021/acsami.8b04046

Xiao, W.Z., Wang, L.L., Xu, L., Li, X.F., Deng, H.Q.: First-principles study of magnetic properties in Ag-doped SnO2. Phys. Status Solidi B **248**, 1961–1966 (2011). https://doi.org/10.1002/pssb.201046567

Xing, G.Z., Yi, J.B., Wang, D.D., Liao, L., Yu, T., Shen, Z.X., et al.: Strong correlation between ferromagnetism and oxygen deficiency in Cr-doped In2O3-δ nanostructures Phys. Rev. B Condens. Matter Mater. Phys. **79**, 174406 (2009a). https://doi.org/10.1103/PhysRevB.79.174406

Xing, G.Z., Wang, D.D., Yi, J.B., Wang, D.D., Liao, L., Yu, T., et al.: Strong correlation between ferromagnetism and oxygen deficiency in Cr-doped In2 O3-δ nanostructures. Phys. Rev. B **79**, 174406 (2009b). https://doi.org/10.1103/PhysRevB.79.174406

Xu, X., Xu, C., Dai, J., Hu, J., Li, F., Zhang, S.: Size dependence of defect-induced room temperature ferromagnetism in undoped ZnO nanoparticles. J. Phys. Chem. C **116**, 8813 (2012). https://doi.org/10.1021/jp3014749

Xu, J., Zhou, Z., Wang, H.: Origin of ferromagnetism in Ru and N codoped TiO_2 nanotubes: experiments and theory investigations. J. Nanomater. **2017**, 2316745 (2017). https://doi.org/10.1155/2017/2316745

Xue, F., Liu, X., Liu, J.: Oxygen vacancy as a medium-induced ferromagnetism in (Fe, Sb) codoped SnO_2 films. J. Phys. Chem. C **123**, 684 (2019). https://doi.org/10.1021/acs.jpcc.8b09662

Xue, D., Song, H., Zhong, X., Wang, J., Zhao, N., Guo, H.: Flexible resistive switching device based on the TiO2 nanorod arrays for non-volatile memory application. J. Alloys Comp. **822**, 153552 (2020). https://doi.org/10.1016/j.jallcom.2019.153552

Yadav, T.P., Shirodkar, S.N., Lertcumfu, N., Radhakrishnan, S., Sayed, F.N., Malviya, K.D., et al.: Chromiteen: a new 2D oxide magnetic material from natural ore. Adv. Mater. Interfaces **5**, 1800549 (2018). https://doi.org/10.1002/admi.201800549

Yakout, S.M.: Robust ferromagnetism and active visible-near infrared photocatalytic properties: Fe based Mn, Co and Ni codoped CuO nanostructures. Opt. Mater. **112**, 110769 (2021a). https://doi.org/10.1016/j.optmat.2020.110769

Yakout, S.M.: Tri-dopants (Mn, Fe, Co): superior room temperature ferromagnetic properties of p-type CuO. Mater. Chem. Phys. **273**, 125110 (2021b). https://doi.org/10.1016/j.matchemphys.2021.125110

Yakout, S.M., El-Sayed, A.M.: Synthesis, structure, and room temperature ferromagnetism of Mn and/or Co doped ZnO nanocrystalline. J. Supercond. Nov. Magn. **29**, 1593 (2016a). https://doi.org/10.1007/s10948-016-3446-x

Yakout, S.M., El-Sayed, A.M.: Structural, morphological and ferromagnetic properties of pure and (Mn, Co) codoped CuO nanostructures. J. Supercond. Nov. Magn. **29**, 2961 (2016b). https://doi.org/10.1007/s10948-016-3641-9

Yan, Z., Ma, Y., Wang, D., Wang, J., Gao, Z., Wang, L.: Impact of annealing on morphology and ferromagnetism of ZnO nanorods. Appl. Phys. Lett. **92**, 081911 (2008). https://doi.org/10.1063/1.2887906

Yan, S., Ou, H., Zhang, L., He, J., Yu, J.: Control of ferromagnetism in $(In_{0.9}Fe_{0.1})_2O_3$ via F doping of electron carriers. Mater. Res. Bull. **61**, 120–123 (2015). https://doi.org/10.1016/j.materresbull.2014.10.005

Yang, T., Song, T.T., Callsen, M., Zhou, J., Chai, J.W., Feng, Y.P.: Atomically thin 2D transition metal oxides: structural reconstruction, interaction with substrates, and potential applications. Adv. Mater. Interfaces **6**, 1801160 (2019). https://doi.org/10.1002/admi.201801160

Ye, X.J., Zhong, W., Xu, M.H., Qi, X.S., Au, C.T., Du, Y.W.: The magnetic property of carbon-doped TiO_2. Phys. Lett. A **373**, 3684 (2009). https://doi.org/10.1016/j.physleta.2009.08.007

Yi, J.B., Lim, C.C., Xing, G.Z., Fan, H.M., Van, L.H., Huang, S.L., et al.: Ferromagnetism in dilute magnetic semiconductors through defect engineering: Li-doped ZnO. Phys. Rev. Lett. **104**, 137201 (2010). https://doi.org/10.1103/physrevlett.104.137201

Yin, X., Wang, Y., Jacobs, R., Shi, Y., Szlufarska, I., Morgan, D., et al.: Massive vacancy concentration yields strong room-temperature ferromagnetism in two-dimensional ZnO. Nano Lett. **19**, 7085 (2019). https://doi.org/10.1021/acs.nanolett.9b02581

Yoo, Y.K., Xue, Q., Lee, H.C., Cheng, S., Xiang, X.D., Dionne, G.F., et al.: Bulk synthesis and high-temperature ferromagnetism of $(In_{1-x}Fe_x)_2O_{3-\sigma}$ with Cu co-doping. Appl. Phys. Lett. **86**, 042506 (2005). https://doi.org/10.1063/1.1854720g

Zhang, C.W., Yan, S.S.: First-principles study on ferromagnetism in Mg-doped. Appl. Phys. Lett. **95**, 232108 (2009). https://doi.org/10.1063/1.3272674

Zhang, J., Qin, Z., Zeng, D., Xie, C.: Metal-oxide-semiconductor based gas sensors: screening, preparation, and integration. Phys. Chem. Chem. Phys. **19**, 6313–6329 (2017). https://doi.org/10.1039/c6cp07799d

Zhang, H., Ouyang, X., Yang, B., Lutes, R., Ni, Y.: Synergistic effect of La and Co co-doping on room-temperature ferromagnetism enhancement of TiO_2 nanoparticles. Ceram. Int. **44**, 6362 (2018). https://doi.org/10.1016/j.ceramint.2018.01.027

Zhang, H., Huang, W., Lin, R., Wang, Y., Long, B., Hu, Q., et al.: Room temperature ferromagnetism in pristine TiO_2 nanoparticles triggered by singly ionized oxygen vacancy induced by calcining in different air pressure. J. Alloys Comp. **860**, 157913 (2021). https://doi.org/10.1016/j.jallcom.2020.157913

Zhou, W., Liu, L., Wu, P.: Nonmagnetic impurities induced magnetism in SnO_2. J. Magn. Magn. Mater. **321**, 3356 (2009). https://doi.org/10.1016/j.jmmm.2009.06.016

Zhou, Y., He, Q., Zhou, F., Liu, Y., Lai, Z., Huang, Y., et al.: Room temperature short-range ferromagnetic order in Ni-doped tetragonal perovskite niobate. Mater. Lett. **305**, 130812 (2021). https://doi.org/10.1016/j.matlet.2021.130812

Zou, C.W., Wang, H.J., Yi, M.L., Li, M., Liu, C.S., Guo, L.P., et al.: Defects related room temperature ferromagnetism in p-type (Mn, Li) co-doped ZnO films deposited by reactive magnetron sputtering. Appl. Surf. Sci. **256**, 2453–2457 (2010). https://doi.org/10.1016/j.apsusc.2009.10.086

Zulfiqar, Z.M., Khan, A., Hua, T., Ilyas, N., Fashu, S., et al.: Oxygen vacancies induced room temperature ferromagnetism and enhanced dielectric properties in Co and Mn co-doped ZnO nanoparticles. J. Mater. Sci. Mater. Electron. **32**, 9463 (2021). https://doi.org/10.1007/s10854-021-05610-5

Publisher's Note Springer Nature remains neutral with regard to jurisdictional claims in published maps and institutional affiliations.

Springer Nature or its licensor (e.g. a society or other partner) holds exclusive rights to this article under a publishing agreement with the author(s) or other rightsholder(s); author self-archiving of the accepted manuscript version of this article is solely governed by the terms of such publishing agreement and applicable law.